

# SANDIA REPORT

SAND87 - 1216 • UC - 13

Unlimited Release

Printed August 1987

## Estimating Payload Internal Temperatures and Radiator Size for Multimegawatt Space Platforms

Dean Dobranich

Prepared by  
Sandia National Laboratories  
Albuquerque, New Mexico 87185 and Livermore, California 94550  
for the United States Department of Energy  
under Contract DE-AC04-76DP00789



***When printing a copy of any digitized SAND Report, you are required to update the markings to current standards.***

Issued by Sandia National Laboratories, operated for the United States Department of Energy by Sandia Corporation.

**NOTICE:** This report was prepared as an account of work sponsored by an agency of the United States Government. Neither the United States Government nor any agency thereof, nor any of their employees, nor any of their contractors, subcontractors, or their employees, makes any warranty, express or implied, or assumes any legal liability or responsibility for the accuracy, completeness, or usefulness of any information, apparatus, product, or process disclosed, or represents that its use would not infringe privately owned rights. Reference herein to any specific commercial product, process, or service by trade name, trademark, manufacturer, or otherwise, does not necessarily constitute or imply its endorsement, recommendation, or favoring by the United States Government, any agency thereof or any of their contractors or subcontractors. The views and opinions expressed herein do not necessarily state or reflect those of the United States Government, any agency thereof or any of their contractors or subcontractors.

Printed in the United States of America  
Available from  
National Technical Information Service  
U.S. Department of Commerce  
5285 Port Royal Road  
Springfield, VA 22161

NTIS price codes  
Printed copy: A04  
Microfiche copy: A01

SAND87-1216  
Unlimited Release  
August 1987

Distribution  
Category UC-13

ESTIMATING PAYLOAD INTERNAL TEMPERATURES AND RADIATOR  
SIZE FOR MULTIMEGAWATT SPACE PLATFORMS

Dean Dobranich

Sandia National Laboratories

ABSTRACT

A conceptual space platform consists of a payload, a power conditioning unit (PCU), and two radiators: the main radiator and a secondary radiator. A computer program was written to determine the required size of the two radiators and the temperatures of the PCU and payload for a given platform power level. An iterative approach is necessary because the required size of the main radiator depends on the size of the secondary radiator and vice versa. Also, the temperatures of the payload and PCU depend on the size of the radiators. The program user can subdivide the two radiators into any number of nodes to increase the accuracy of the radiant heat transfer solution. The use of more nodes also allows better prediction of the nonlinear temperature drop that occurs across the radiators as the working fluid deposits the platform's waste heat in the radiator. View factor expressions are automatically calculated for different choices of the number of nodes. The user can also select different separation distances between the various platform structures. A model is included to couple the radiant and conduction heat transfer that occurs between the payload and its meteoroid shell and between the PCU and its shell. Also, the program allows the use of a refrigerator to cool the payload. If a refrigerator is used, the program determines the amount of additional thermal power needed to run the refrigerator. The results of parametric calculations are included to demonstrate the use of the program.

# CONTENTS

	PAGE
1.0 INTRODUCTION .....	1
2.0 MATHEMATICAL MODELS .....	5
2.1 Radiosity Equations .....	5
2.2 Radiator Sizing Equations .....	8
2.3 View Factors .....	12
2.4 Coupled Heat Transfer Modes .....	15
2.5 Refrigerator Model .....	19
3.0 COMPUTER PROGRAM APPLICATION .....	20
3.1 Example Input and Output .....	20
3.2 Radiator Nodes .....	21
3.3 Conduction .....	26
3.4 Separation Distance .....	28
3.5 Convection .....	31
3.6 Refrigerators .....	33
3.7 Payload Temperature .....	33
4.0 SUMMARY AND CONCLUSIONS .....	35
5.0 REFERENCES .....	36
APPENDIX A - ASSESSMENT PROBLEMS .....	37
APPENDIX B - COMPUTER PROGRAM LISTING .....	39
APPENDIX C - SAMPLE PROGRAM OUTPUT .....	54

## 1.0 INTRODUCTION

Proposed multimegawatt (MMW) space-based platforms containing payloads of electronic equipment will require large amounts of electrical power for operation. The consumption of electrical power by the payload will result in the generation of waste heat which must be rejected to space, via radiant heat transfer, to keep the operating temperatures of the equipment within acceptable limits. An active cooling system can be used to cool the electronic equipment whereby a working fluid is pumped through a heat exchanger within the payload and then to an external (secondary) radiator. The size of the required secondary radiator will depend on several factors including the amount of waste heat to be rejected, the operation temperature of the radiator, and the proximity of the radiator to other platform components such as the payload and the power supply (main) radiator.

Determining the size of the secondary radiator is not straightforward because the presence of all of the major platform structures must be considered when performing the radiant heat transfer calculations. Figure 1.1 provides a schematic diagram of the four major structures comprising the platform. The four structures are (1) the main radiator, (2) the secondary radiator, (3) the power conditioning unit (PCU) and its shell, and (4) the payload and its shell.

The main and secondary radiators are represented as disks facing each other and separated by some specified distance. A disk radiating from both sides represents the most effective use of heat transfer area for a single radiator. However, if more than one radiator along with other relatively hot components are included on the platform, this configuration will not provide the most effective use of radiating area. Besides the relative radiator orientation, the optimum radiator configuration depends on other factors such as platform stability, maneuverability, survivability, and structural considerations. (The design of such a platform will certainly be a complicated and challenging endeavor.) The platform configuration used for the analyses described in this report was chosen for modeling simplicity and to demonstrate that the position of the platform components relative to each other strongly affects the radiant heat transfer calculations. These effects are demonstrated by varying the component separation distances in the radiant heat transfer calculations.

The main radiator must reject the waste heat associated with the primary power source of the platform. Most likely, a Brayton or Rankine thermodynamic cycle will be used for the thermal-to-electric conversion. The thermal-to-electric conversion efficiency will therefore be on the order of 20% to 30% and most of the primary power will be converted to waste heat. For a Brayton cycle, the temperature at which power is rejected to space is not constant, thereby further complicating the task of determining the radiator sizes.

The secondary radiator, as already mentioned, is required to remove the waste heat associated with the cooling of the electronic components comprising the PCU and payload. The fluid inlet temperature to this radiator is equal to the outlet temperature of the heat exchanger cooling the electronic components. Likewise, the fluid outlet temperature of the radiator is equal to the inlet temperature of the heat exchanger. For cooling of the electronic components, the temperature of the secondary radiator working fluid can not exceed the temperature of the components being cooled (unless a refrigerator is used). Thus, operation of the components at higher temperatures allows reduction of the secondary radiator area in two ways. First, less waste heat needs to be rejected actively to maintain a higher payload temperature, and second, the inlet and outlet temperatures of the secondary radiator can be higher.

The PCU and PCU shell are both modeled as cylinders with the outer cylinder representing the shell. The PCU consists of the electronic components required to convert the platform electrical power into a form which the payload can use. These components typically are about 95% efficient and thus a relatively small amount of waste heat will be generated within the PCU.

The payload and its shell are geometrically modeled the same way as the PCU and its shell. The payload consists of electronic equipment required for the operation of the platform such as computers, radars, radios, and guidance systems. Essentially all the electrical power consumed by these components will be converted to waste heat (with the possible exception of the radars). Active cooling of these components will therefore be essential.

Modeling all the electrical equipment as a single payload is based on the simplification that the different electronic components operate at the same temperature. In reality, each component will have different temperature limitations and may even require its own radiator.

Surrounding the PCU and payload will be shells. These shells serve two purposes: (1) to provide protection of the internal components from meteoroids, and (2) to provide additional surface area for radiation of waste heat to space. Thus, the PCU and payload each have a "shell radiator" surrounding them. Transfer of heat from the internals to the shell will occur by radiation and via conduction through any support structure. Also, heat pipes (which have very high effective conductivities) may be connected between the shell and the internals to take maximum advantage of the additional shell surface area.

A computer program has been written to model the heat transfer between the major structures of this conceptual space platform. Because the heat flux across the radiators will vary

with position, the program allows the user to divide the radiators into any number of nodes. Because view factors for all the surfaces of the platform cannot be determined until the sizes of the radiators are known, an iterative approach is used to solve for the radiator dimensions. Also, the maximum temperature at which the secondary radiator can operate depends on the temperatures of the PCU and payload. Again, an iterative scheme is used to determine this temperature. If a refrigerator is used to cool the payload, the program determines the additional thermal power required to run the refrigerator along with the resulting increase in the main radiator size. Finally, heat transfer from the PCU or payload to the PCU or payload shell will occur both by radiation and by conduction. Coupling of the two modes of heat transfer is accomplished by using the Modified Regula Falsi method for finding roots of a function.

This report contains a description of the models used in the program to determine the radiator sizes and the PCU and payload temperatures. Also, the results of parametric calculations are presented to demonstrate the heat transfer dependence on various input parameters such as the number of nodes, the separation distances between the various structures, the conduction parameters, and the use of a refrigerator.

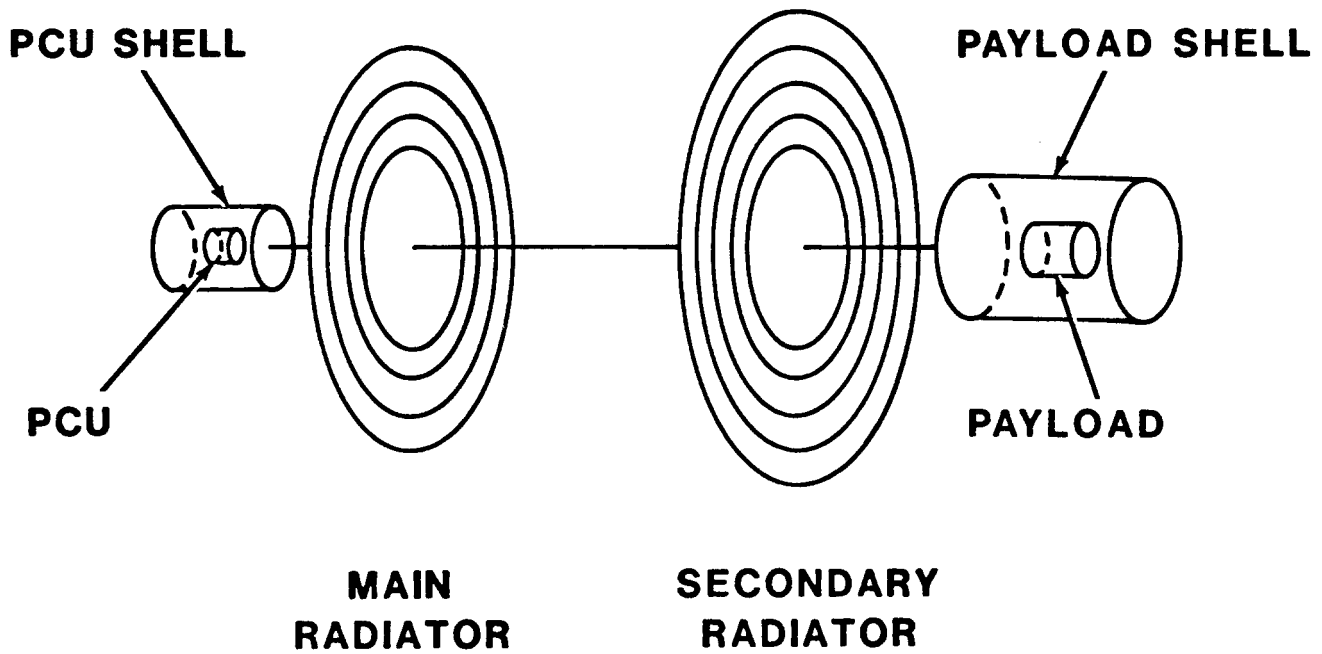


Figure 1.1 Schematic Diagram of Platform Structures

## 2.0 MATHEMATICAL MODELS

### 2.1 Radiosity Equations

The first step toward determination of the radiator sizes and the payload and PCU temperatures is the development of a model to calculate the radiant heat transfer between multiple surfaces. For this model, the assumption has been made that all the surfaces are gray and diffuse. A gray surface is one whose radiative properties (i.e., emissivity) are not a function of wavelength. A diffuse surface is one that emits and reflects radiation with equal intensity in all directions. The first assumption is reasonable for this model because most of the radiation will be emitted at relatively long wavelengths. The radiation properties for the surfaces of interest do not vary much at these long wavelengths. The second assumption is adopted because the directional characteristics of the surfaces simply are not known. The use of these two assumptions offers considerable simplification of the radiant heat transfer equations and is consistent with the level of accuracy required keeping in mind the conceptual nature of the space platform. (Such a platform has never been built or designed.)

To model the radiant heat transfer between the surfaces, a method known as the radiosity method [1] was used. This method, common in the literature, allows the calculation of radiant heat transfer between any number of surfaces. The radiosity of a surface is defined as the rate at which radiation leaves a surface by both emission and reflection. For  $N$  surfaces, a linear set of  $N$  equations with  $N$  unknowns is solved to determine the radiosity for each surface. From the radiosities, the heat flux or temperature can be determined for the surfaces.

Three types of surfaces are considered in the radiosity method: (1) surfaces for which the temperature is known, (2) surfaces for which the net heat flux is known, and (3) "two-sided" surfaces. A two-sided surface is one in which the temperatures of both sides of the surface are equal, although unknown. Also, the sum of the heat fluxes from both sides of the surface is known; however, the heat flux for each side is unknown. An example of a two-sided surface is a structure radiating to space (a radiator) with the sun shining on only one side. Thus, the heat flux leaving each side of the radiator is unknown even though the total heat produced by the radiator is known. If heat conduction from one side of the radiator to the other is very large (i.e., low thermal resistance), the two sides will have the same temperature; however, this temperature is unknown.

The equations relating the radiosity for one surface to the radiosity of all the other surfaces are derived in reference 1 for surface types 1 and 2; i.e., surfaces with either known temperature or net heat flux. These equations are given below.

$$\sigma T_i^4 = \frac{J_i}{\epsilon_i} - \left( \frac{1-\epsilon_i}{\epsilon_i} \right) \sum_j F_{ij} J_j \quad (1)$$

$$\frac{q_i}{A_i} = J_i - \sum_j F_{ij} J_j \quad (2)$$

where:  $J_i$  = radiosity for surface  $i$ ,  
 $T_i$  = temperature for surface  $i$ ,  
 $q_i/A_i$  = heat flux for surface  $i$ ,  
 $\epsilon_i$  = emissivity for surface  $i$ ,  
 $F_{ij}$  = view factor from surface  $i$  to surface  $j$ , and  
 $\sigma$  = Stefan-Boltzmann constant.

The equations for surface type 3, a two-sided surface, are derived below starting with equations (1) and (2) along with the additional constraints that:

$$T_i = T_k \quad (3)$$

and,

$$Q = q_i + q_k \quad (4)$$

The subscripts  $i$  and  $k$  refer to the two sides of the surface. In the matrix of radiosity equations, each side of a two-sided surface is represented as a separate surface. Therefore, information indicating what surfaces are "connected" to form a two-sided surface must be provided within the program.

First, equation (1) is written for both sides of the two-sided surface,  $i$  and  $k$ . These two equations can then be combined, using the first constraint given above (equation 3), to eliminate the unknown temperatures. Thus,

$$\frac{J_i}{\epsilon_i} - \left( \frac{1-\epsilon_i}{\epsilon_i} \right) \sum_j F_{ij} J_j = \frac{J_k}{\epsilon_k} - \left( \frac{1-\epsilon_k}{\epsilon_k} \right) \sum_j F_{kj} J_j \quad (5)$$

Now, equation (2) is written for both sides of the surface and the second constraint (equation 4) is used to eliminate the unknown heat fluxes. Also note that the areas of both sides are equal and recall that  $Q$  is the total heat produced by the two-sided surface. Thus,

$$\frac{Q}{A} = J_i - \sum_j F_{ij} J_j + J_k - \sum_j F_{kj} J_j \quad (6)$$

Equations (5) and (6) are now rewritten such that the radiosity for the  $i^{\text{th}}$  surface is isolated on the left side of the equal sign and all other terms are placed on the right. (This is done to place the equations in a form suitable for use with a Gauss-Siedel iterative scheme and to simplify the derivation.) The new equations are:

$$J_i = B \left[ \frac{J_k}{\epsilon_k} + \left( \frac{1}{\epsilon_i} - 1 \right) \sum_{j \neq i} F_{ij} J_j - \left( \frac{1}{\epsilon_k} - 1 \right) \sum_{j \neq i} F_{kj} J_j \right] \quad (5')$$

$$J_i = G \left[ \frac{Q}{A_i} - J_k + \sum_{j \neq i} (F_{ij} + F_{kj}) J_j \right] \quad (6')$$

These summations are over all surfaces except the  $i^{\text{th}}$  surface because this term has been factored out. It is necessary to satisfy both the temperature and the heat flux constraints simultaneously for both sides of the two-sided surface. Therefore, equation (6') is written for the  $k^{\text{th}}$  surface and then substituted into equation (5') to yield a single equation for the radiosity of the  $i^{\text{th}}$  surface. After simplification and rearrangement:

$$J_i = B \left[ \left( \frac{1}{\epsilon_i} - 1 \right) \sum_{j \neq i} F_{ij} J_j - \left( \frac{1}{\epsilon_k} - 1 \right) \sum_{j \neq i} F_{kj} J_j + \right. \quad (7)$$

$$\left. \frac{G}{\epsilon_k} \frac{Q_i}{A_i} + \frac{G}{\epsilon_k} \sum_{j \neq k} (F_{ij} + F_{kj}) J_j \right] / \left[ 1 + \frac{B G}{\epsilon_k} \right]$$

where:

$$B = 1 / \left[ \frac{1}{\epsilon_i} - F_{ii} \left( \frac{1}{\epsilon_i} - 1 \right) \right] \cdot G = 1 / (1 - F_{kk})$$

Thus, equations (1), (2), and (7) can be used to determine the radiosities for surfaces within an enclosure containing surface types 1, 2, and 3, respectively. As already mentioned, a Gauss-Siedel iterative technique was chosen to solve these equations. In this technique, the initial radiosities for all surfaces are guessed. Using these initial values, new values are

calculated for each surface with the updated value used for each successive radiosity calculation. With this technique, any desired accuracy (which should be consistent with the accuracy of the radiation properties) can be chosen for the desired convergence criteria.

These equations were programmed for computer application in a subroutine called RADHT. Because of the generality with which the equations are written, it is possible to use this subroutine to solve for the radiation heat transfer within any enclosure simply by changing the input to the subroutine. To lend some confidence in the use of this subroutine, several assessment calculations were performed. The problems for these calculations were taken from various textbooks and are presented in Appendix A. Very good agreement with the textbook solutions was achieved for all cases.

## 2.2 Radiator Sizing Equations

The platform radiators have been assumed to be contact heat exchangers as discussed in reference 2. In a contact heat exchanger, a working fluid flowing in conduits transfers waste heat to heat pipes which are "plugged into" the conduit. The heat pipes then radiate the waste heat to space. For the disk radiators in this study, the conduits are like the spokes of a wheel and the heat pipes are connected circumferentially to form the disk. In a contact radiator, the contact resistance between the conduit and the heat pipes can be made very small such that the temperature drop across the contact can be considered insignificant. Also, the temperature drop from the working fluid to the conduit wall is typically less than 5 K [2]. Thus, very efficient use of the heat transfer area can be achieved. For the purposes of determining radiator size, the temperature drop from the fluid to the heat pipes was assumed to be zero. Because this temperature drop is really nonzero, the actual radiator size would be somewhat larger.

The input to subroutine RADHT, discussed in the previous section, includes the view factors between all the different surfaces of the enclosure. The problem arises that the view factors can not be determined until the dimensions of the radiators are known. To further complicate this problem is the fact that the temperature distribution from the inside edge to the outside edge of each disk radiator is also not known. This section includes a discussion of an iterative approach to solve this problem.

First, consider a radiator in the shape of a disk. Assuming  $T = T_1 = T_2$ , an energy balance on a differential area element,  $dA$ , of the radiator yields:

$$\dot{m}C_p dT = \left[ \sigma \epsilon_1 (T_1^4 - T_{s1}^4) + \sigma \epsilon_2 (T_2^4 - T_{s2}^4) \right] dA \quad (8)$$

where:  $\epsilon_1$  = surface emissivity of side 1,  
 $\epsilon_2$  = surface emissivity of side 2,  
 $T_1$  = surface temperature of side 1,  
 $T_2$  = surface temperature of side 2,  
 $T_{s1}$  = effective background temperature, side 1,  
 $T_{s2}$  = effective background temperature, side 2,  
 $\sigma$  = Stefan-Boltzmann constant.  
 $\dot{m}$  = working fluid mass flow rate, and  
 $c_p$  = working fluid specific heat.

The boundary conditions for this differential equation are the radiator inlet and outlet temperatures which are program input values. The required value for the quantity  $\dot{m}c_p$  can thus be determined as the heat to be rejected divided by the inlet to outlet temperature difference.

Therefore, for steady-state operation, the energy deposited in the differential area element by the radiator working fluid must equal the energy radiated from both sides of the radiator. The solution of this equation yields the temperature distribution across the radiator. The key to solving this equation is in finding an effective background temperature,  $T_s$ , that accounts for the presence of all the structures of the platform.

This equation can be simplified by making some algebraic substitutions. First, for the disk:

$$dA = 2\pi r dr$$

where  $r$  is the radius.

Also,

$$\bar{\epsilon} = (\epsilon_1 + \epsilon_2)/2.0$$

$$C = -\dot{m}c_p/4\pi\bar{\epsilon}\sigma$$

$$T_s^4 = (\epsilon_1 T_{s1}^4 + \epsilon_2 T_{s2}^4)/(\epsilon_1 + \epsilon_2)$$

This last substitution allows the replacement of two variables by a single variable. This implies that it is possible to determine a single effective background temperature for both sides of the element; i.e., it is not necessary to determine the effective background temperature for each side separately. This substitution considerably simplifies the solution because fewer variables are required and less computation per iteration is needed. Also, an analytical solution to the integral can be found. Without this substitution, the integration would have to be performed numerically.

These substitutions result in the following equation:

$$rdr = \left( \frac{C}{T_s^4 - T^4} \right) dT \quad (9)$$

The solution to this differential equation can be determined by the integration of each side of the equation over the appropriate intervals. Thus,

$$\int_{R_I}^{R_O} rdr = \int_{T_I}^{T_O} \left( \frac{C}{T_s^4 - T^4} \right) dT \quad (10)$$

where:  $R_I$  = the disk inner radius,  
 $R_O$  = the disk outer radius,  
 $T_I$  = the temperature at the inner radius, and  
 $T_O$  = the temperature at the outer radius.

Performing the integration yields:

$$\frac{r_{i+1}^2}{2} = \frac{r_i^2}{2} + \frac{C}{4T_{si}^3} \left[ \ln \left\{ \frac{(T_{si} + T_{i+1})}{(T_{si} - T_{i+1})} \frac{(T_{si} - T_i)}{(T_{si} + T_i)} \right\} + 2 \left\{ \arctan \left( \frac{T_{i+1}}{T_{si}} \right) - \arctan \left( \frac{T_i}{T_{si}} \right) \right\} \right] \quad (11)$$

If the disk is subdivided into  $N$  nodes, equation (11) can be applied to each node where the subscripts  $i$  and  $i+1$  refer to the inner and outer boundary of the node, respectively.

At this point, two different solution approaches could be used. The first approach is to use equation (11) to determine the outer radius of the radiator for a given value of  $T_s$ . (The inner radius, inside temperature, and outside temperature are known.) Now the radiator can be divided into  $N$  nodes of any arbitrary width. Equation (11) can then be used to solve for the temperatures at the boundaries of the nodes. These temperatures must be solved iteratively due to the transcendental nature of the equation. A simpler approach (the approach used in the program) is to assume that the node widths will be such that the temperature drop across all nodes is equal. Thus,

$$T_{i+1} = T_i + (T_I - T_O)/N$$

Now, equation (11) can be used to solve for the node radii directly. This approach has the additional benefit of automatically placing more nodes in the region of the largest temperature gradient.

With the node radii and end temperatures thus computed, it is necessary to determine an "average" temperature for each node. This average is not the algebraic average of the node end temperatures because of the fourth power temperature dependence for radiant heat transfer. To determine the average node temperature, consider an energy balance on the node.

$$\dot{m}c_p(T_i - T_{i+1}) = 2\sigma\bar{\epsilon}\pi(r_{i+1}^2 - r_i^2)(\bar{T}_i^4 - T_{si}^4) \quad (12)$$

where  $\bar{T}_i$  is the average temperature that satisfies this equation. Rearranging this equation yields:

$$\bar{T}_i = \left[ \frac{2C(T_{i+1} - T_i)}{r_{i+1}^2 - r_i^2} + T_{si}^4 \right]^{1/4} \quad (12')$$

Now equation (10) can be used to determine the radius at which the average temperature occurs. To do this, perform the integration with  $r_i$  as the upper limit of integration for  $r$  and  $T_i$  as the upper limit of integration for  $T$ .

Thus, equations (11) and (12') can be used to determine the dimensions and temperature distribution of the radiator for a given effective background temperature,  $T_{s,i}$ , for each node. The task now is to determine the  $T_s$  values for both radiators. The following iterative procedure is used to accomplish this task.

STEP 1: Use the effective temperature of space as a first guess to  $T_s$  for each node.

STEP 2: Use equations (11) and (12') to determine the node radii and temperatures.

STEP 3: Now that values for the radiator dimensions exist, view factors for all the surfaces of the platform can be calculated. Also, values for the average node temperatures exist. Therefore, the subroutine RADHT can be used to determine the heat fluxes and temperatures for all surfaces.

STEP 4: Now calculate the power radiated away by both sides of each node using the RADHT calculated values of heat flux. Thus,

$$P_i = q_i + q_k \quad (13)$$

where the  $q$ 's are the product of the node heat flux and area. The  $i$  and  $k$  subscripts indicate the two sides of the node. Now, for each node,

$$P_i = 2A_i\sigma\bar{\epsilon}(\bar{T}_i^4 - T_{s,i}^4) \quad (14)$$

Rearranging yields an expression for updating the values of  $T_s$ ,

$$T_{s,i}' = (\bar{T}_i^4 - P_i/A_i 2 \sigma \bar{\epsilon})^{1/4} \quad (14')$$

STEP 5: Now, the updated values of  $T_s$  can be compared to the previous values. Steps 1 through 4 can then be repeated until these values converge or when the  $P_i$  values converge to the desired degree of accuracy.

Use of the Gauss-Siedel iterative technique for solving the radiosity equations fits in well with this procedure because the radiosities from the previous iteration can be used for the initial guess for the current iteration.

Subroutine RADSIZE contains the logic to perform the radiator-sizing calculations. The subroutine has been written to allow the radiator inlet temperature to be at either the inside or outside radius of the radiator. As will be discussed later, it may be advantageous (with respect to minimizing required radiator area) to deliver the hot working fluid to the outside of the radiator first, via insulated conduits, and to then collect the cooler fluid at the inner radius.

If the radiator is to reject heat at a constant temperature (as would be the case for a Rankine cycle main power supply), the radiator inlet and outlet temperatures are equal and thus the temperature distribution across the radiator is known. For this case, the preceding procedure is simplified. Now, equation (14) can be used to solve for the node areas directly because the node temperatures are known. However, the effective background node temperatures remain as unknowns and the iterative approach is still required.

### 2.3 View Factors

It is necessary to calculate view factors between all surfaces of the platform. This is done in subroutines VIEW1 and VIEW2. Subroutine VIEW1 determines the view factors between the payload and PCU and their shells. The view factors between these structures need to be calculated only once because the dimensions for these structures are fixed. Subroutine VIEW2 determines the view factors between all the nodes of the two radiators and all other surfaces. Because the dimensions of the radiators are determined iteratively, it is necessary to recalculate these view factors for each iteration.

Both view factor subroutines make use of only two basic view factor expressions. All other view factors are determined by view factor algebra or by using the fact that the sum of the view factors from one surface to all the others must equal 1.0.

The two basic view factor expressions are for a disk-to-disk and a cylinder-to-concentric-cylinder. The expressions for the two view factors are taken from reference 3. A considerable amount of view factor algebra is required to arrive at expressions for view factors between cylinders and rings and between rings and other rings. Figure 2.3.1 provides schematic diagrams of the different geometries for which view factors are calculated. Subroutines VIEW1 and VIEW2 make use of other subroutines and functions to calculate all the required view factors. The following is a list of these subroutines and functions.

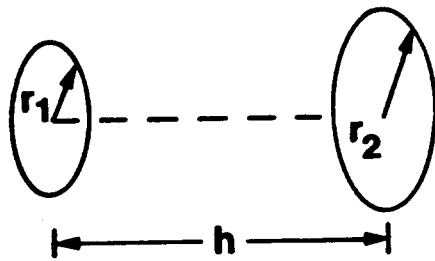
FUNCTION DTOD - determines the view factor between a disk of radius  $r_1$  to another disk of radius  $r_2$  separated by distance  $h$ . (See reference 3, page 826, #21.)

FUNCTION CTOD - determines the view factor between a cylinder of radius  $r_1$  and an adjacent and perpendicular disk of radius  $r_2$ . Some view factor algebra is included starting with the view factor between two concentric cylinders. (See reference 3, page 828, #28.)

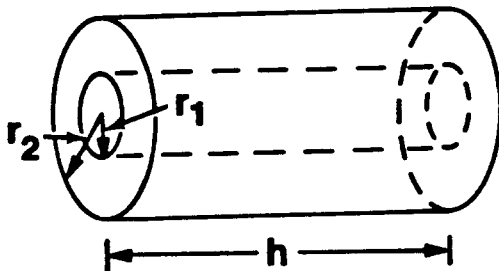
SUBROUTINE FRINGS - uses function DTOD and view factor algebra to determine ring-to-ring view factors. The rings are separated by distance  $h$ .

SUBROUTINE CTORING - uses function CTOD and view factor algebra to determine cylinder-to-ring view factors. The cylinder and ring are separated by distance  $h$ .

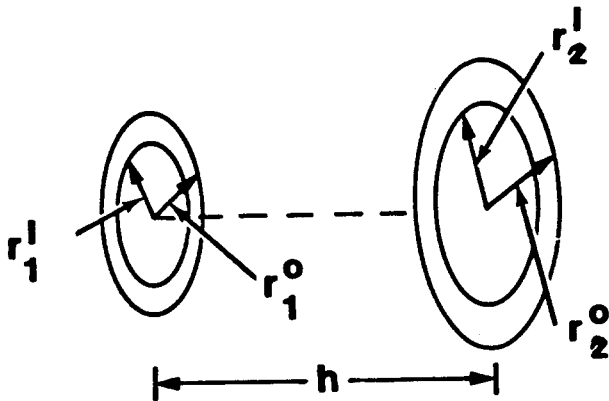
Because the radiators can be divided into any number of nodes, the view factor subroutines must be written with the number of nodes as a parameter. The details of the bookkeeping and the view factor algebra used to arrive at all the view factors will not be explained in any further detail. However, Appendix B, which contains a computer listing of the entire program, can be examined for the appropriate FORTRAN expressions.



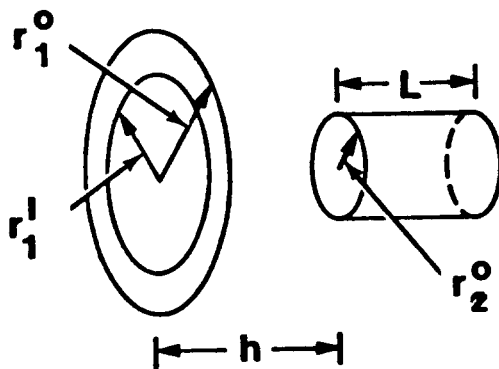
Disk-to-Disk



Cylinder-to-Concentric Cylinder



Ring-to-Ring



Cylinder-to-Ring

Figure 2.3.1 View Factor Geometries

## 2.4 Coupled Heat Transfer Modes

The radiator-sizing equations discussed in the previous sections can be solved without considering conduction between the payload (or PCU) internals and the shell because only the total heat flux leaving the shell is of consequence for radiator sizing. In other words, it doesn't matter if the waste heat generated in the internals is transferred to the shell by conduction or radiation; it is the total heat transferred that determines the shell temperature and heat flux. Therefore, the radiator-sizing calculations can be performed assuming that all the waste heat is transferred from the internals to the shell by radiation and that none of the waste heat is transferred to the shell by conduction. However, determining the temperature of the internals does depend on the amount of waste heat removed by conduction and radiation.

Waste heat generated in the PCU and payload internals will be transferred from the internals to the shell by both radiation and conduction. The conduction will occur along the support structure used to support the shell. Also, heat pipes may be connected between the internals and shell to greatly improve this heat transfer mechanism. Heat pipes have very large effective thermal conductivities and essentially can transfer heat isothermally. The coupling of the conduction and radiation heat transfer modes is nonlinear because conduction is proportional to the first power of temperature; whereas, radiation is proportional to the fourth power. To accomplish this coupling, use was made of the Modified Regula Falsi [4] method for finding roots of a function. This coupling approach is discussed in this section.

An energy balance on the internals can be written as:

$$q - q_v - q_d - q_r = 0.0 \quad (15)$$

where:  $q$  = total waste heat generated,  
 $q_v$  = waste heat removed by convection,  
 $q_d$  = waste heat removed by conduction, and  
 $q_r$  = waste heat removed by radiation.

The expression for the convection term depends on the type of heat exchanger used to cool the internals; i.e., the number of fluid passes, the size and type of fins, etc. Given the conceptual nature of the platform, convection heat transfer is not modeled in detail. Instead, the convection term is treated parametrically such that  $q_v$  is assumed to be a known quantity. (The convection term will be discussed in more detail later in this section.) Thus, two terms in equation (15) are unknown, namely,  $q_d$  and  $q_r$ . Equation (15) can be rewritten in the form of a function as:

$$f(q_r) = q - q_v - q_d - q_r \quad (15')$$

Finding the values of  $q_r$  and  $q_d$  that make this function equal to zero is desired. This is equivalent to finding the root of an equation for which the Modified Regula Falsi method is applicable.

To evaluate the radiation term, the radiosity equations of Section 2.1 can be used for the internals and shell surfaces. Solution of the equations yields the shell and internal temperatures from which the conduction term can be calculated using:

$$q_d = (kA/x) \Delta T$$

where:  $k$  = effective thermal conductivity,  
 $A$  = heat transfer area for conduction,  
 $x$  = conduction path length, and  
 $\Delta T$  = temperature drop from internals to shell.

Thus,  $q_d$  is a function of the unknown internals temperature which is a function of  $q_r$ . Choosing  $q_r = 0.0$  (i.e., all the waste heat is removed from the internals by conduction) and  $q_r = q - q_v$  (i.e., all the waste heat is removed by radiation) provides an interval containing a root that satisfies equation (15'). Starting with this interval, the Modified Regula Falsi method quickly finds the root and thus the internals temperature. This is equivalent to solving the radiation and conduction equations simultaneously. However, use of the Modified Regula Falsi method allows one to keep the expressions for conduction and radiation separate. A graphical depiction of this process is shown in Figure 2.4.1. The program was written such that either the  $kA/x$  value or the  $\Delta T$  value can be input. If  $\Delta T$  is input, the required  $kA/x$  value to achieve this  $\Delta T$  is calculated.

Returning to the convection term, recall that  $q_v$  was treated as a known quantity. To obtain an order of magnitude estimate of the  $hA$  value required to remove the specified amount of waste heat, Newton's law of cooling can be used. The waste heat removed by convection is thus expressed as:

$$q_v = hA(T - T_c) \tag{16}$$

where:  $h$  = effective heat transfer coefficient,  
 $A$  = total heat transfer area available,  
 $T$  = temperature of the internals, and  
 $T_c$  = average coolant temperature.

An estimate of the value of  $T_c$  is made using the algebraic average of the heat exchanger inlet and outlet temperatures. Note that for heat transfer from the internals to the fluid, the fluid temperature must be less than the internals temperature. Also, recall that the outlet temperature of the heat exchanger

is equal to the inlet temperature of the secondary radiator. The inlet temperature of the secondary radiator must be known before the radiator can be sized. Therefore, a guess is made for this temperature and the radiator-sizing calculations and conduction-convection coupling calculations are performed. An updated value is then calculated based on the calculated temperature of the internals. Thus,

$$\begin{aligned}T_I &= T - \Delta t_{\min} \\T_O &= T_I + \Delta T\end{aligned}$$

where:  $T_I$  = the secondary radiator inlet temperature (equivalent to the heat exchanger outlet temperature),  
 $T_O$  = the secondary radiator outlet temperature (equivalent to the heat exchanger inlet temperature),  
 $\Delta T$  = the desired radiator temperature difference,  
 $T$  = the internals temperature, and  
 $\Delta t_{\min}$  = the minimum allowed temperature difference between the internals and cooling fluid.

Figure 2.4.2 graphically demonstrates the relationship between the various temperatures. The updated values of  $T_I$  and  $T_O$  are then used to repeat the radiator sizing and internal temperature calculations.

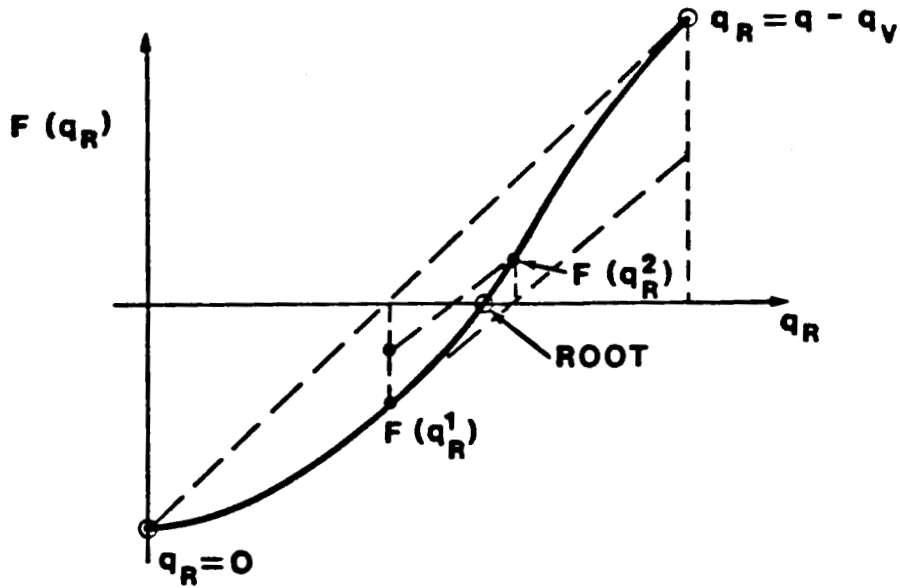


Figure 2.4.1 The Root of the Conduction-Radiation Equation

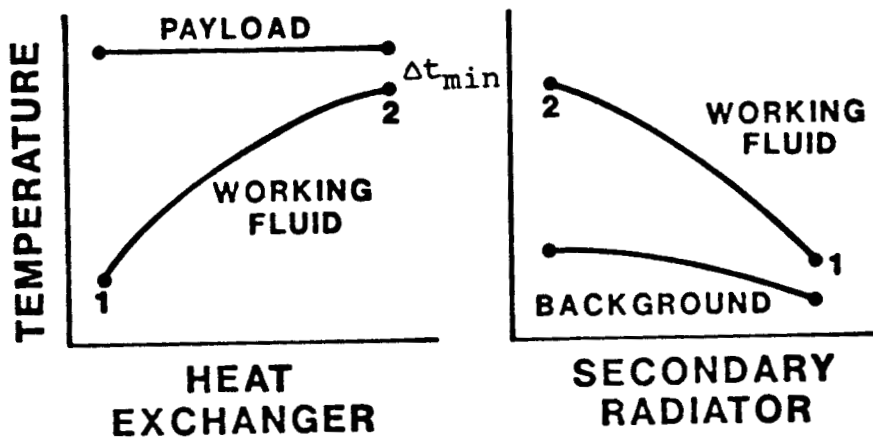


Figure 2.4.2 Radiator and Internal Temperature Relationship

## 2.5 Refrigerator Model

The computer program has been written so that the use of a refrigerator to cool the payload internals can be investigated. The possible benefit of a refrigerator is that it allows the rejection of payload waste heat at a temperature higher than the payload, thereby decreasing the size of the required secondary radiator. However, because additional power is required to run the refrigerator, more waste heat associated with the main power supply will be generated necessitating a larger main radiator.

The refrigerator coefficient of performance (COP) is calculated as some specified fraction of the Carnot COP. The Carnot COP ( $COP_C$ ) is calculated as:

$$COP_C = T_1 / (T_h - T_1) \quad (17)$$

where:  $T_1$  = the lowest temperature of the working fluid,  
and  
 $T_h$  = the highest temperature of the working fluid.

The secondary radiator is assumed to operate at  $T_h$ . The working fluid is assumed to operate at the payload temperature minus some specified payload-to-working fluid temperature difference. Because the payload temperature is unknown, an iterative procedure is employed to determine the value of  $T_1$  such that  $T_1$  equals the calculated payload temperature minus the specified payload-to-working fluid temperature difference.

The amount of electric power needed to power the refrigerator,  $W$ , is determined as  $Q$  divided by COP where  $Q$  is the amount of waste heat to be removed by the refrigerator. (The waste heat associated with the refrigerator is not included in the payload waste heat.) The amount of additional thermal power required is found as  $W$  divided by the thermal-to-electric power conversion efficiency. An increase in the power supply increases the amount of waste heat to be rejected by the main radiator. Thus, the required size of the main radiator must be updated each iteration.

### 3.0 COMPUTER PROGRAM APPLICATION

#### 3.1 Example Input and Output

To demonstrate the use and capabilities of the computer program, several parametric calculations were performed. This section includes a description of these calculations. An annotated example input file is given in Table 3.1.1. The annotations provide a concise description of the required input variables. This example input provides a "base case" on which all subsequent parametric calculations are based. The resulting program output for this example problem is provided in Appendix C. Only three nodes for the main radiator and four nodes for the secondary radiator were used to keep the output relatively short.

Table 3.1.1 Sample Program Input

15	MAXIMUM ITERATIONS FOR RADIATOR SIZING (- FOR DEBUG)
0.01	RADIATOR-SIZING RELATIVE CONVERGENCE CRITERIA
20	MAXIMUM ITERATIONS FOR GAUSS-SIEDEL SOLUTION
0.005	GAUSS-SIEDEL RELATIVE CONVERGENCE CRITERIA
3	NUMBER OF MAIN RADIATOR NODES
4	NUMBER OF SECONDARY RADIATOR NODES
0.90	EMISSIVITY OF LEFT SIDE OF MAIN RADIATOR
0.90	EMISSIVITY OF RIGHT SIDE OF MAIN RADIATOR
0.90	EMISSIVITY OF LEFT SIDE OF SECONDARY RADIATOR
0.90	EMISSIVITY OF RIGHT SIDE OF SECONDARY RADIATOR
0.9.0.9.0.9	EMISSIVITY OF INSIDE OF PCU SHELL (LEFT.CENTER.RIGHT)
0.9.0.9.0.9	EMISSIVITY OF OUTSIDE OF PCU SHELL (LEFT.CENTER.RIGHT)
0.9.0.9.0.9	EMISSIVITY OF INSIDE OF PAYLOAD SHELL (LEFT.CENTER.RIGHT)
0.9.0.9.0.9	EMISSIVITY OF OUTSIDE OF PAYLOAD SHELL (LEFT.CENTER.RIGHT)
0.80	EMISSIVITY OF PCU
0.80	EMISSIVITY OF PAYLOAD
300.0	EFFECTIVE TEMPERATURE OF SPACE (K)
480.0	TEMPERATURE AT INNER RADIUS OF MAIN RADIATOR (K)
985.0	TEMPERATURE AT OUTER RADIUS OF MAIN RADIATOR (K)
470.0	TEMPERATURE AT INNER RADIUS OF SECONDARY RADIATOR (K)
400.0	TEMPERATURE AT OUTER RADIUS OF SECONDARY RADIATOR (K)
6.0	INNER RADIUS OF MAIN RADIATOR (M)
7.0	INNER RADIUS OF SECONDARY RADIATOR (M)
1.0	SEPARATION DISTANCE BETWEEN PCU AND MAIN RADIATOR (M)
30.0	SEPARATION DISTANCE BETWEEN MAIN AND SEC RADIATOR (M)
1.0	SEPARATION DISTANCE BETWEEN SEC RADIATOR AND PAYLOAD (M)
8.0	DIAMETER OF PCU SHELL (M)
12.0	LENGTH OF PCU SHELL (M)
10.0	DIAMETER OF PAYLOAD SHELL (M)
15.0	LENGTH OF PAYLOAD SHELL (M)
6.0	DIAMETER OF PCU (M)
10.0	LENGTH OF PCU (M)
8.0	DIAMETER OF PAYLOAD (M)
12.0	LENGTH OF PAYLOAD (M)
40.0E6	TOTAL PLATFORM THERMAL POWER (W)
0.25	THERMAL-TO-ELECTRIC CONVERSION EFFICIENCY
0.0	FRACTION OF CARNOT REFRIGERATOR COP (IF 0.0, NO REFRIGERATOR)
0.05	FRACTION OF ELECTRIC POWER CONVERTED TO PCU WASTE HEAT
0.0	FRACTION OF PCU WASTE HEAT REMOVED ACTIVELY (TO SEC RAD)
0.9	FRACTION OF ELECTRIC POWER CONVERTED TO PAYLOAD WASTE HEAT
0.9	FRACTION OF PAYLOAD WASTE HEAT REMOVED ACTIVELY (SEC RAD)
-5.0	MIN DELTA-T BETWEEN PAYLOAD AND SEC RAD WORKING FLUID *
-2.0	KA X (-) OR DESIRED DELTA-T (-) FOR PCU SHELL CONDUCTION
-2.0	KA X (-) OR DESIRED DELTA-T (-) FOR PAYLOAD SHELL CONDUCTION

- \* IF 0, VARIABLE NOT USED AND THE INPUT VALUES FOR SECONDARY RADIATOR INLET AND OUTLET TEMPERATURE ARE USED AS INPUT (NO ITERATION). IF A REFRIGERATOR IS USED, THIS IS THE TEMPERATURE DIFFERENCE BETWEEN THE PAYLOAD AND THE REFRIGERATOR WORKING FLUID.

The first page of the output provides information concerning the nodes of the two radiators, such as the node radius, area, temperature, and the effective background temperature for each node. This information is calculated by subroutine RADSIZE. The next page provides the final output, such as radiator areas, and PCU and payload temperatures. The third page provides surface identification numbers for all the surfaces used in the radiant heat transfer solution as computed in subroutine RADHT. Next is a list of the view factors between all the surfaces. Even with only a few nodes for each radiator, there are 841 view factors for this example problem. Many of these view factors are zero, however, and are not printed. The last page of output displays the results of the final call to subroutine RADHT; this includes the radiosities for each of the 29 surfaces.

### 3.2 Radiator Nodes

The number of nodes used for each radiator affects the final calculated radiator area with the greater number of nodes providing the more accurate results. Table 3.2.1 shows the effect of varying the number of nodes in the secondary radiator (the number of nodes in the main radiator is held constant) for two different values of waste heat delivered to the secondary radiator. This demonstrates that the choice of the number of nodes depends on the particular problem being solved; thus, care should be taken in selecting an appropriate number of radiator nodes. (The separation distance between the two radiators was also found to have a big influence on the number of nodes required.)

Table 3.2.1 Effect of the Number of Radiator Nodes

Waste Heat = 8.1 MW

# Nodes	Secondary Radiator Area (m <sup>2</sup> )
3	6198
6	6093
12	6078
20	6075

Waste Heat = 4.5 MW

# Nodes	Secondary Radiator Area (m <sup>2</sup> )
6	3905
12	3042
20	2976
30	2966

Figure 3.2.1 demonstrates the convergence of the effective background temperature used in determining radiator size. Twelve nodes were used in the secondary radiator for this example. The initial guess for the effective background temperature for each node was 300 K. The values of the twelve node temperatures for the next three iterations (the curves labeled 2, 3, and 4) show

that convergence occurs after some oscillations. Originally, the oscillations were even more severe. To dampen the oscillations, the updated  $T_S$  values were modified according to:

$$T_S = w T_S(\text{current}) + (1-w) T_S(\text{previous})$$

where  $w$  was chosen to be 0.8. This relaxation value, determined by trial and error, was found to work reasonably well for most problems.

Table 3.2.2 shows information related to the iterations required to determine the radiator sizes. In this table,  $L$  is the radiator-sizing iteration number and  $M$  is the number of iterations required for the radiosity equations (subroutine RADHT) to converge. The total power is the sum of all the node powers. For this example, the desired main radiator total power was 30.0 MW and the desired secondary radiator total power was 8.1 MW. Thus, the radiator sizing iterative scheme converges rapidly for this problem.

Table 3.2.2 Iteration Summary

L	M	Maximum Node Power Relative Error	Total Power (main radiator)	Total Power (sec radiator)
1	9	0.7261	28.71 MW	2.489 MW
2	4	0.3110	29.16 MW	10.450 MW
3	2	0.1309	30.00 MW	7.864 MW
4	1	0.0074	30.00 MW	8.090 MW

All of the calculations discussed in this section are based on the use of an effective temperature of space equal to 300 K. (The effective temperature of space should not be confused with the effective background temperature which accounts for the presence of all platform structures and space.) The effective space temperature accounts for the radiation arriving from the sun (directly or reflected off the earth) along with the radiation emitted by the earth. This value is a function of platform orientation, altitude, orbit inclination, geometry, and surface-coating properties and can be expected to range anywhere from 200 K to 360 K for anticipated platform applications. The value of 300 K was chosen as a representative intermediate value.

Figures 3.2.2 and 3.2.3 show the main and secondary radiator temperatures, respectively. The main radiator has 10 nodes and the secondary radiator has 12 nodes. Also, the radiators are 30 m apart. The fluid inlet to the main radiator was chosen to be at the outer radius of the disk while the inlet for the secondary radiator is at the inner radius. This arrangement resulted in the smallest total radiator area. If the inlet to

the secondary radiator is reversed, the cooler nodes close to the inner radius do not reject heat very well because the presence of the hot main radiator and payload shell result in a very high effective background temperature for those nodes. An alternative to reversing the flow direction would be to increase the inner radius of the secondary radiator, thereby effectively moving the radiator away from the other platform structures.

The effective background temperature for the main radiator nodes is relatively flat indicating that the other surfaces of the platform do not have a significant impact on the main radiator's ability to reject heat. This is because the main radiator operates at a high temperature compared to other surfaces. The effective background temperature for the secondary radiator nodes, however, is large relative to the radiator temperature because the temperatures of the other surfaces of the platform are relatively high. These two figures also show that the temperature distributions of the two radiators are completely different. This is due to the different relative influence of each platform surface on each radiator because of their different spatial orientations. Changing the flow direction, the PCU and payload sizes, and the platform structure separation distances all have significant impact on the radiator temperature distribution.

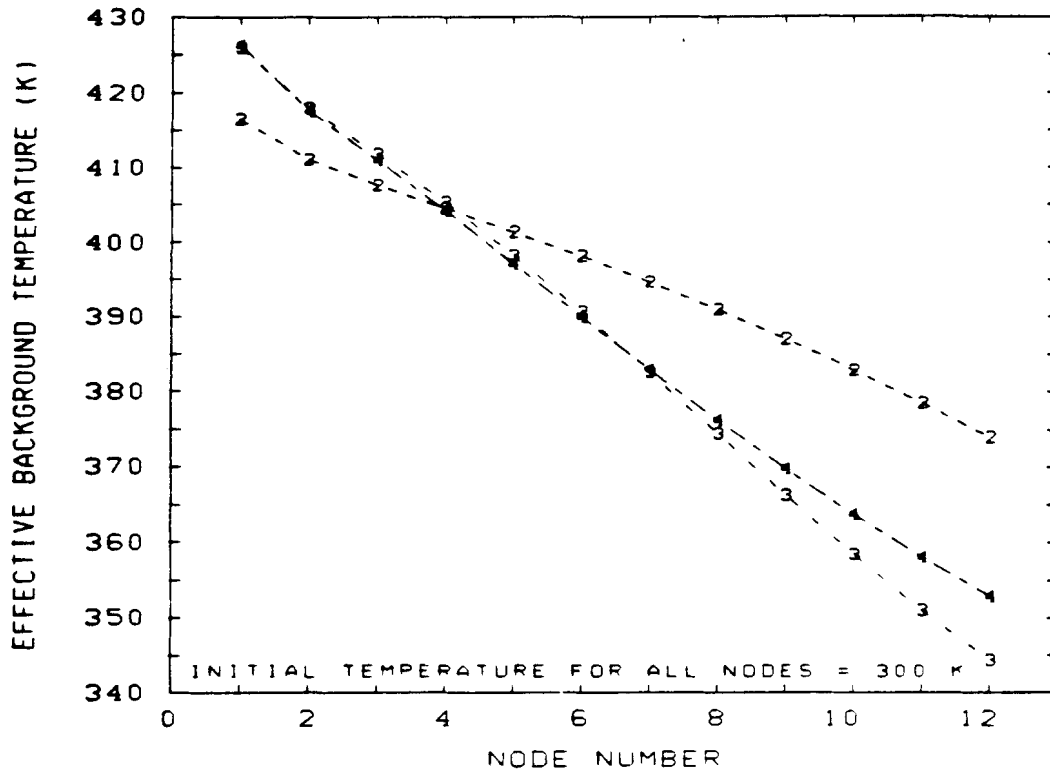


Figure 3.2.1 Radiator Sizing Iterations

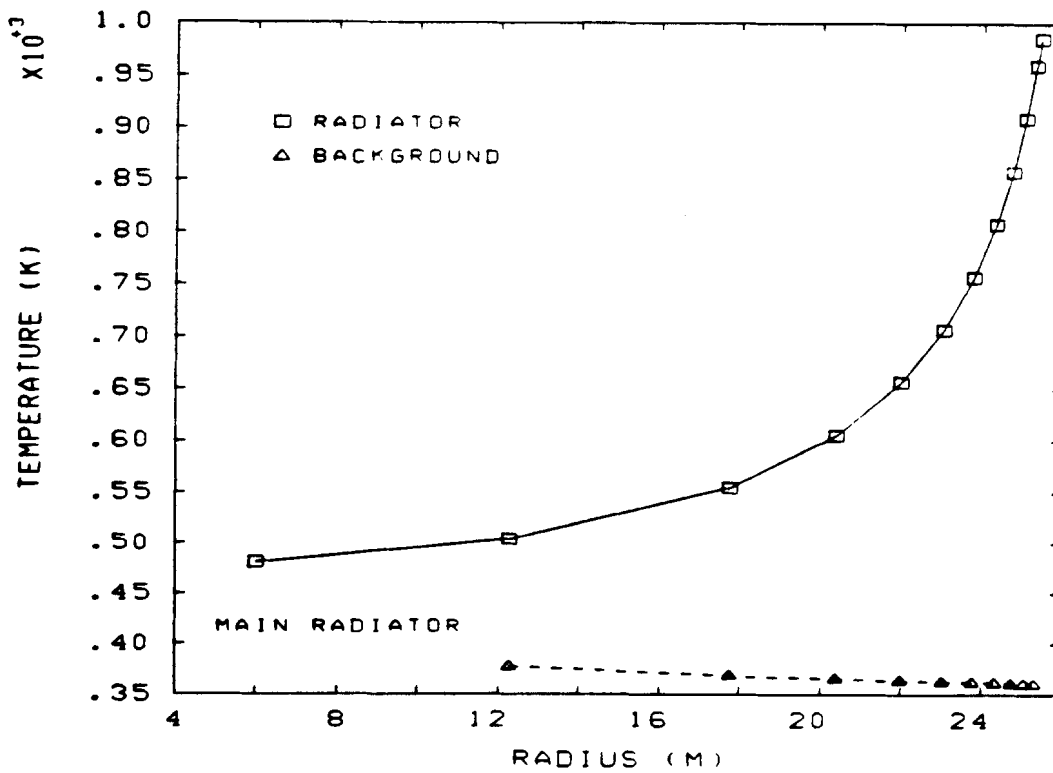


Figure 3.2.2 Main Radiator Temperature Distribution

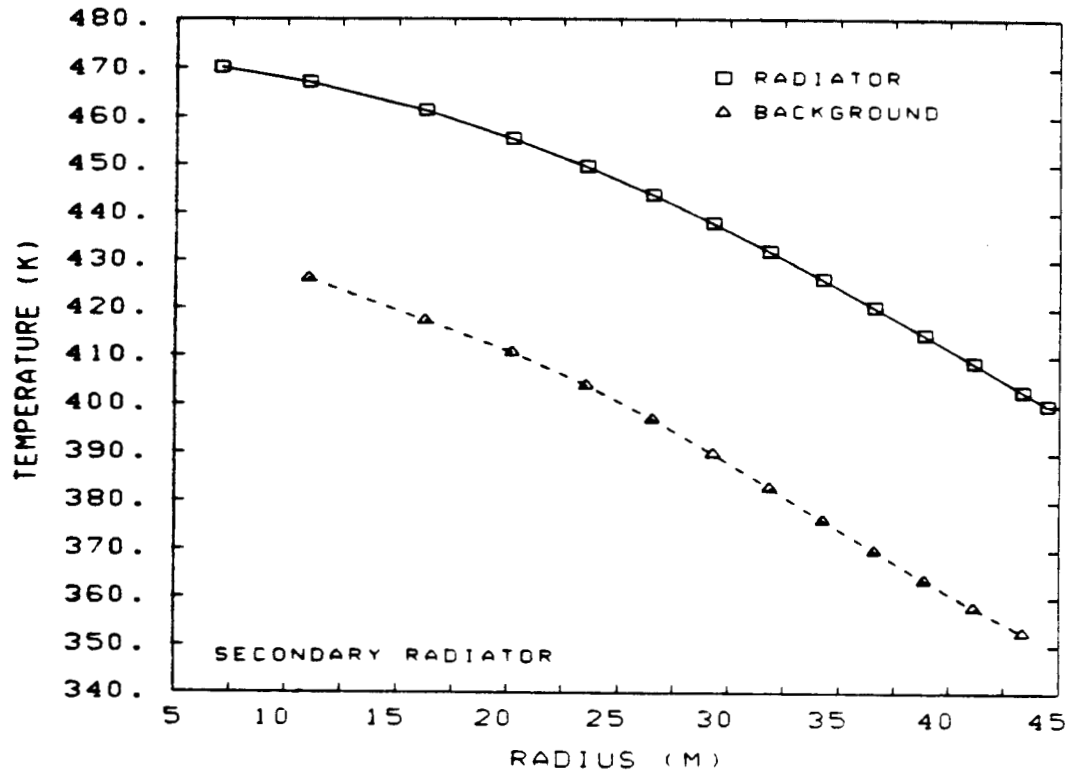


Figure 3.2.3 Secondary Radiator Temperature Distribution

### 3.3 Conduction

Figure 3.3.1 shows the effect of payload-to-shell conduction on the payload temperature. It is not clear if sufficient room would exist for enough heat pipes to achieve the  $kA/x$  values shown on this curve. However, a set of parametric calculations was performed to show the possible benefit of using heat pipes to remove payload waste heat. The payload temperature drops very rapidly as the  $kA/x$  value is increased. It is clear that without any heat pipes the payload temperature would be much higher.

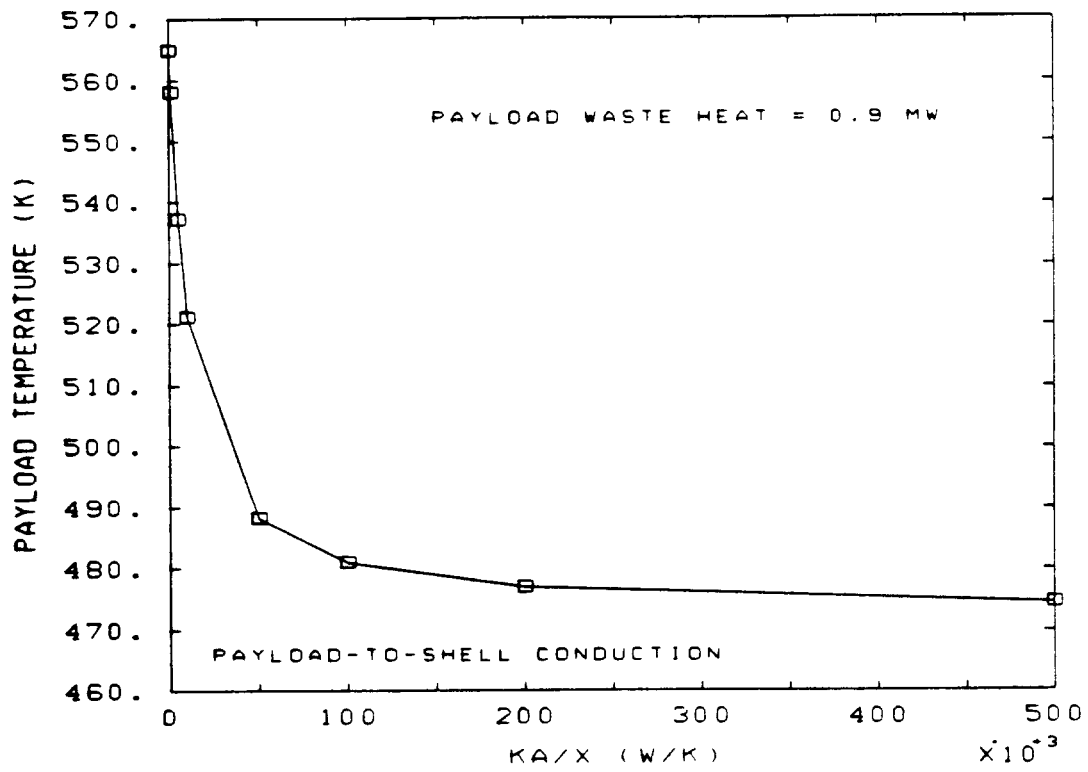


Figure 3.3.1 Payload-to-Shell Conduction

### 3.4 Separation Distance

The geometric parameter that has the most effect on the size of the radiators is the separation distance between the main and secondary radiators. This effect is demonstrated in Figure 3.4.1 which shows the secondary radiator area as a function of separation distance for two different amounts of waste heat delivered to the secondary radiator. It is apparent that increasing the separation distance greatly reduces the required size of the radiator. The size of the main radiator (not shown on the Figure) varies between 2300 m<sup>2</sup> and 1550 m<sup>2</sup> for separation distances from 10 m to 300 m. The effect of separation distance on the main radiator is not as significant because it operates at a much higher temperature than the secondary radiator. However, if the operating temperature of the secondary radiator is increased or the temperature of the main radiator decreased, the effect on the main radiator size would become more significant.

The radiator separation distance also influences the PCU and payload temperatures as shown in Figure 3.4.2. The payload temperature is affected more because the hot main radiator has the largest influence on the payloads ability to radiate waste heat to space.

Another parameter that affects the size of the radiators and the payload and PCU temperatures is the separation distance between the shells (PCU and payload) and the radiators. (To show this effect, a radiator-to-radiator separation distance of 500 m was used; thus, the radiators are far enough apart to preclude any influence on each other.) Figure 3.4.3 shows the effect of varying these separation distances on the radiator areas. The reason the radiator areas increase for separation distances from about 2 m to 10 m is that more of the shell views the adjacent radiator in this range of separation distances. At zero separation distance, only the curved surface of the shell views the adjacent radiator. As the separation distance is increased, one end of the shell also begins to view the radiator, resulting in an overall increase in the shell-to-radiator view. Further increases in the separation distance result in an overall decrease of this view such that the required radiator area decreases. A similar effect on payload and PCU temperatures is shown in Figure 3.4.4.

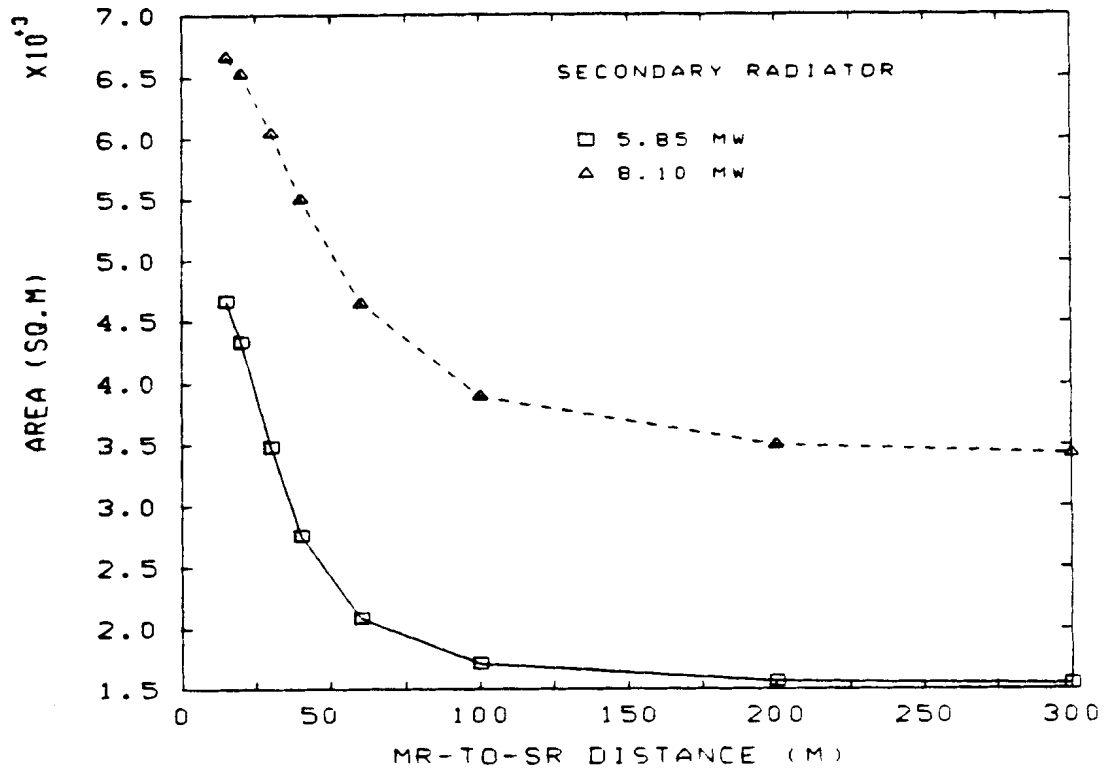


Figure 3.4.1 Radiator Area Versus Separation Distance

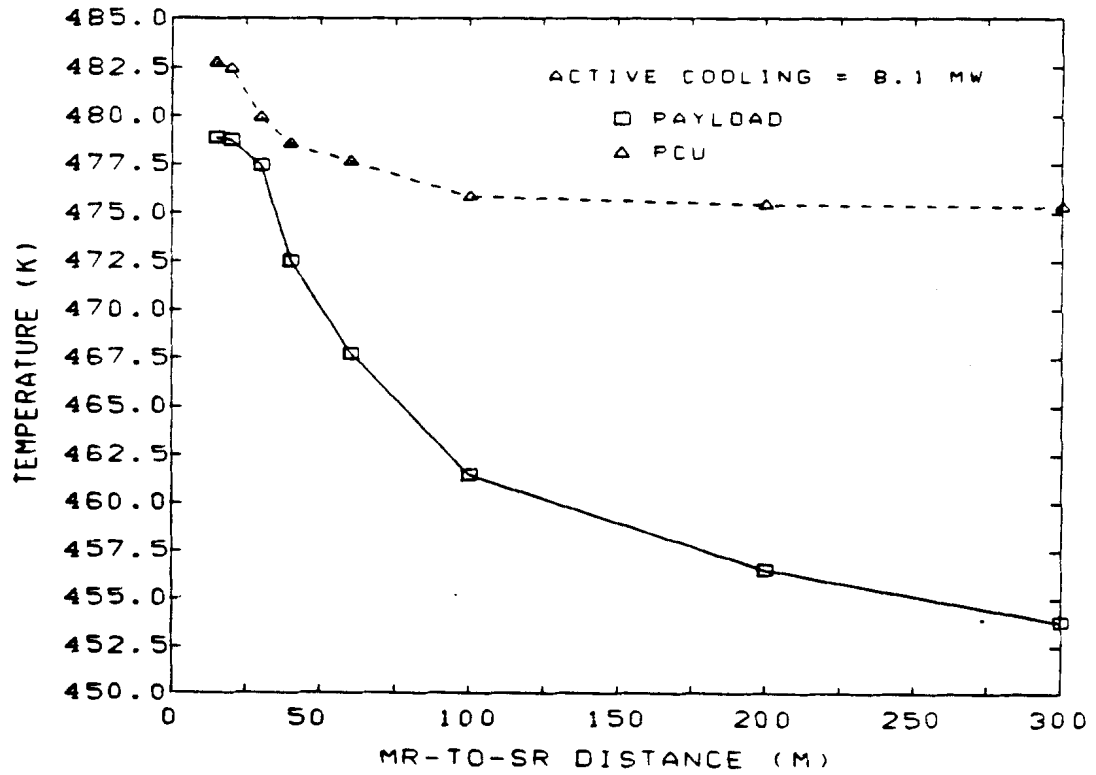


Figure 3.4.2 Temperature Versus Radiator Separation Distance

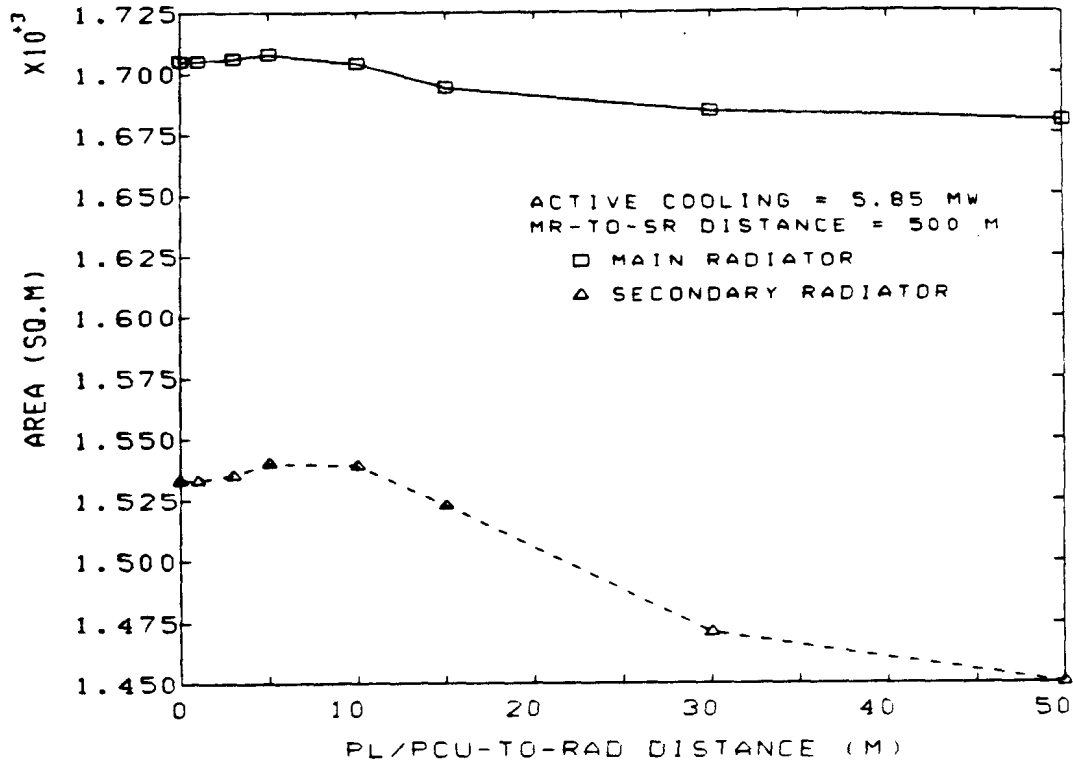


Figure 3.4.3 Radiator Area Versus Shell-to-Radiator Distance

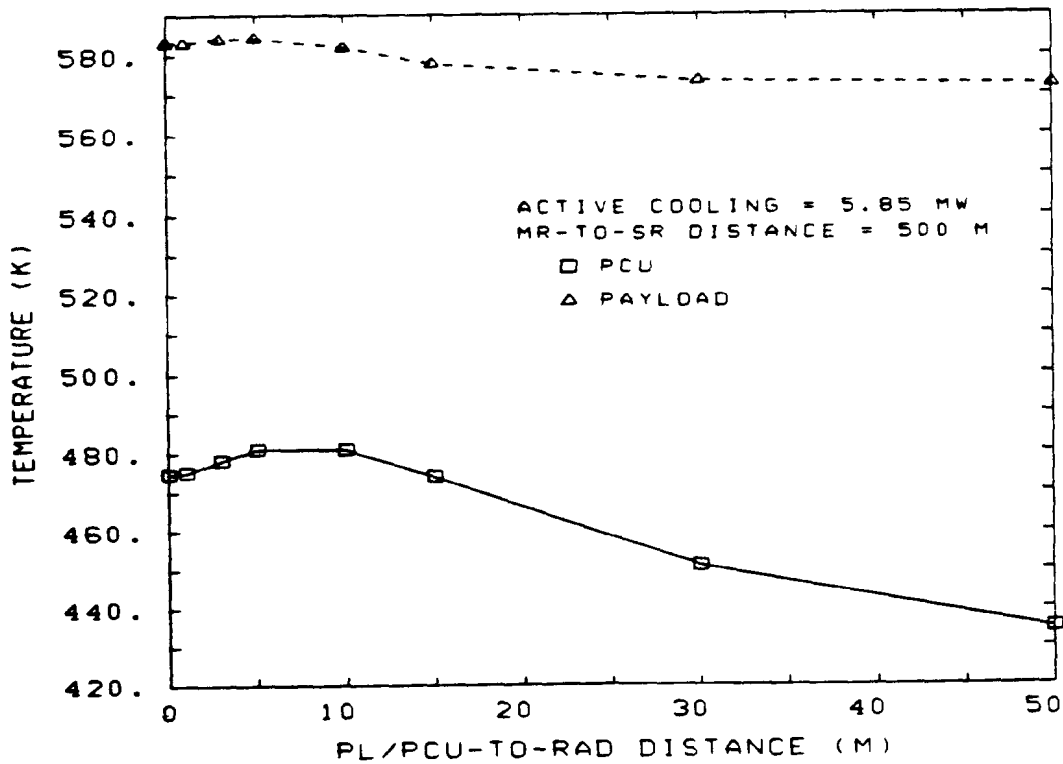


Figure 3.4.4 Temperature Versus Shell-to-Radiator Distance

### 3.5 Convection

One of the output variables of the computer program is an estimate of the value of  $hA$  required for convective cooling of the payload. For a given working fluid and flow rate, an estimate of  $h$  can be made; using the estimated  $hA$  and  $h$  values, the heat transfer area can be determined. This crude estimate can at least be used to provide some idea of the area required by the heat exchanger to actively cool the payload. Figure 3.5.1 shows the effect of different  $hA$  values on the payload temperature. Increasing the value of  $hA$  has a diminishing influence on the temperature because the temperature difference between the working fluid and the payload decreases as more and more heat is removed from the payload.

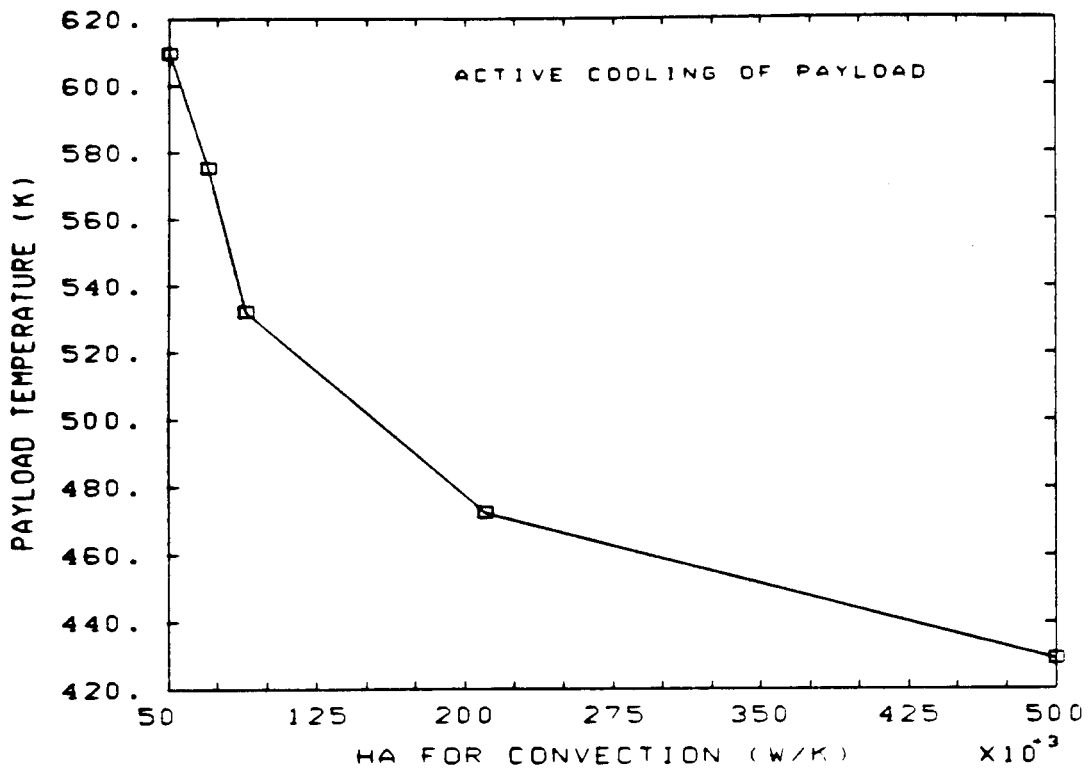


Figure 3.5.1 Effect of Convection on Payload Temperature

### 3.6 Refrigerators

The effect of a refrigerator was determined by repeating the base case, specifying a refrigerator COP of 70% of the Carnot COP. Also, the secondary radiator was assumed to operate at 700 K and the temperature difference between the payload and the refrigerator working fluid was taken as 40 K. (In the base case without a refrigerator, the log mean temperature difference between the payload and the payload heat exchanger working fluid was also approximately 40 K.) The results indicate that a 6 MWe refrigerator is needed to cool the payload, requiring an additional 24 MW of thermal power. Compared to the base case, the size of the secondary radiator decreased from 6087 m<sup>2</sup> to 395 m<sup>2</sup> while the main radiator increased in size from 1906 m<sup>2</sup> to 2967 m<sup>2</sup>.

### 3.7 Payload Temperature

The principal motivation for creating this radiant heat transfer computer program was to estimate the reduction in secondary radiator area that could be achieved by allowing higher payload and PCU operating temperatures. Electronic components capable of high temperature operation require less active cooling. Also, higher component temperatures allow rejection of waste heat at higher temperature by the secondary radiator. The relationship between the secondary radiator area and payload temperature is provided in Figure 3.7.1 for the base case input parameters. This curve shows that increasing the permissible payload temperature from 450 K to 600 K results in over a factor of two reduction in the radiator area.

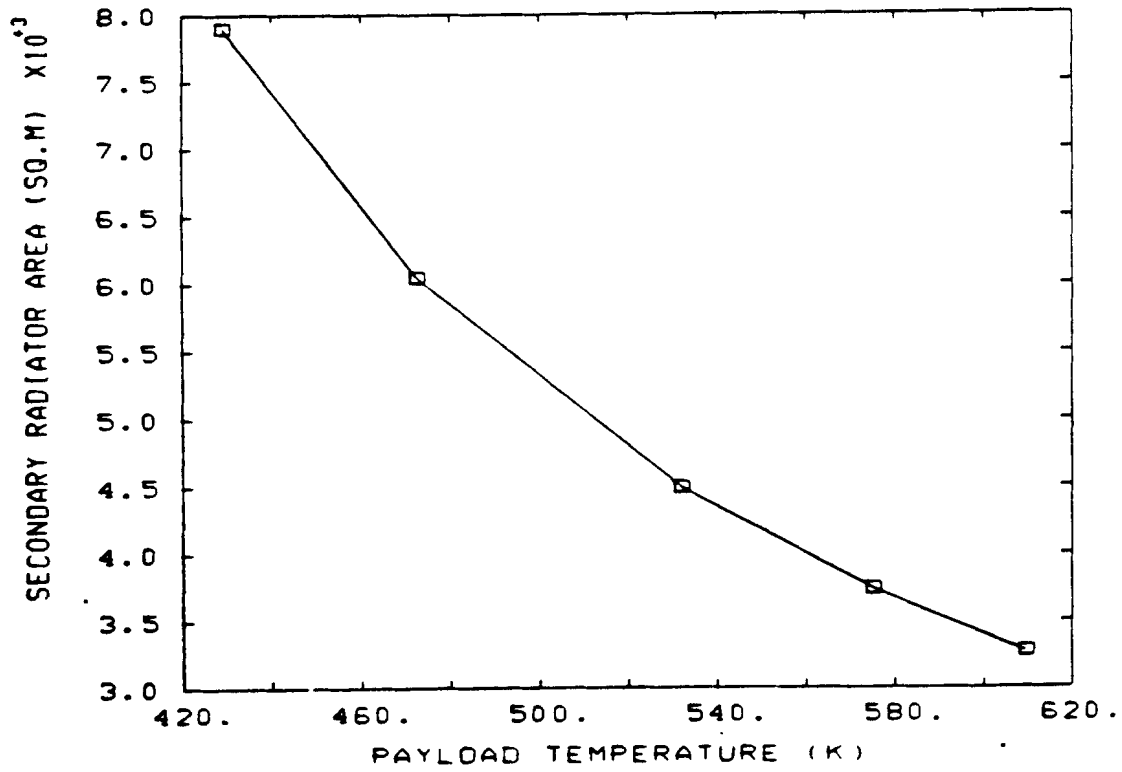


Figure 3.7.1 Effect of Payload Temperature on Radiator Area

#### 4.0 SUMMARY AND CONCLUSIONS

A conceptual space platform consists of a payload, a PCU, and two radiators: the main radiator and a secondary radiator. A computer program was written to determine the required size of the two radiators and the temperatures of the PCU and payload for a given platform power level. The program includes a model for the radiant heat transfer between the various platform surfaces. An iterative algorithm is employed in conjunction with this model to determine the size of the radiators. The program user can subdivide the two radiators into any number of nodes to increase the accuracy of the radiant heat transfer solution. The use of more nodes also allows better prediction of the nonlinear temperature drop that occurs across the radiators as the working fluid deposits the platform's waste heat in the radiator. View factor expressions are automatically calculated for different choices of the number of nodes. The user can also select different separation distances between the various platform structures. A model is included to couple the radiant and conduction heat transfer that occurs between the payload and its shell and between the PCU and its shell. Also, the program allows the use of a refrigerator to cool the payload. If a refrigerator is used, the program determines the amount of additional thermal power needed to run the refrigerator.

This computer program was used to perform a variety of parametric calculations. The results indicate that the secondary radiator size is strongly dependent on its proximity to the main radiator and that the radiant interchange that occurs between the various platform structures has a large effect on the structure temperatures. The size of the secondary radiator also depends on the amount of waste heat that it must radiate to space and the temperature at which it operates. Use of a refrigerator to cool the payload significantly reduces the size of the secondary radiator but at the expense of increased main radiator and power supply size. Results of this computer program indicate that with or without a refrigerator, the use of high temperature electrical components in the PCU and payload can significantly reduce the required size of the secondary radiator by allowing a reduction in the amount of waste heat to be removed and by allowing an increase in the inlet and outlet temperatures of the radiator.

The calculations in this report were included to demonstrate the intended use of the program. In order to perform these calculations for a conceptual space platform it was necessary to assume values for many of the program input variables. It should be noted that there are a lot of variables to consider and that the results can only indicate trends in the various functional relationships. Assuming representative variable values and performing parametric calculations is the best one can do until a detailed platform design has been completed.

## 5.0 REFERENCES

1. Holman, J. P., Heat Transfer, Fourth Edition, (McGraw-Hill Book Company, 1976).
2. Howell, H. R., Development of a Contact Heat Exchanger for a Constructable Radiator System, Vought Corp., Report # 2-53200/3R-53490, NASA-CR-171730, July, 1983.
3. Seigel, R. and J. R. Howell, Thermal Radiation Heat Transfer, Second Edition, (McGraw-Hill Book Company, 1981).
4. S. D. Conte and C. de Boor, Elementary Numerical Analysis, (McGraw-Hill Book Company, 1972).

APPENDIX A - ASSESSMENT PROBLEMS

SAMPLE PROBLEM (1) - CYLINDRICAL CAVITY AT CONSTANT TEMPERATURE REJECTING HEAT TO BLACKBODY SINK AT 293.3 K

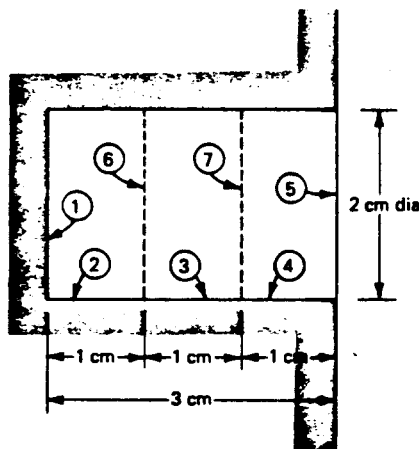
RADIATION ANALYSIS

SURFACE	EMISSIVITY	TEMPERATURE (KELVIN)	QNETPP (W/SQ.M)	RADIOSITY (W/SQ.M)	TEXTBOOK [1] RADIOSITY (W/SQ.M)
1	0.60000	1273.30	0.13282E+05	0.14016E+06	0.14003E+06
2	0.60000	1273.30	0.84339E+04	0.14339E+06	0.14326E+06
3	0.60000	1273.30	0.15274E+05	0.13883E+06	0.13872E+06
4	0.60000	1273.30	0.34994E+05	0.12569E+06	0.12557E+05
5	1.00000	293.30	-.11659E+06	0.41952E+03	0.41952E+06

SAMPLE PROBLEM (2) - CYLINDRICAL CAVITY WITH SURFACE 1 AT 1273.3 K, WITH SURFACES 2,3, AND 4 INSULATED ( $Q''=0.0$ ), REJECTING HEAT TO BLACKBODY SINK OF 293.3 K

RADIATION ANALYSIS

SURFACE	EMISSIVITY	TEMPERATURE (KELVIN)	QNETPP (W/SQ.M)	RADIOSITY (W/SQ.M)	TEXTBOOK [1] RADIOSITY (W/SQ.M)
1	0.60000	1273.30	0.50442E+05	0.11539E+06	0.11532E+05
2	0.60000	1093.27	0.00000E+00	0.80988E+05	0.81019E+05
3	0.60000	1004.92	0.00000E+00	0.57815E+05	0.57885E+05
4	0.60000	884.84	0.00000E+00	0.34751E+05	0.34767E+05
5	1.00000	293.30	-.38822E+05	0.41952E+03	0.41952E+05



SAMPLE PROBLEM (3)

(PROBLEM 16, PAGE 278 OF REFERENCE [3])

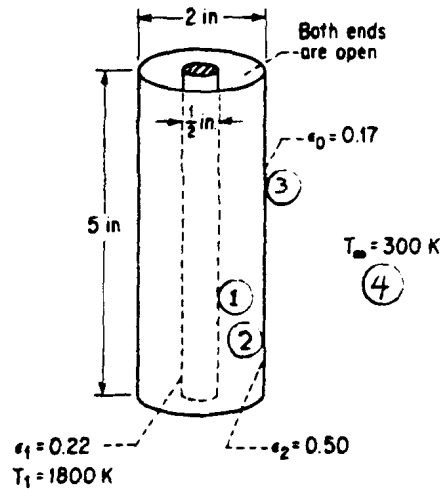
TWO CONCENTRIC CYLINDERS, INNER CYLINDER AT 1800 K,  
ENVIRONMENT AT 300 K

THIS PROBLEM TESTS THE TWO-SIDED SURFACE OPTION IN SUBROUTINE RADHT  
TEXT BOOK [3] TEMPERATURE OF SURFACES 2,3 (OUTER CYLINDER) = 1048 K

NUMBER OF ITERATIONS = 15  
(RELATIVE ERROR = 1.0000E-03)

RADIATION ANALYSIS FOR ALL SURFACES

SURFACE	EMISSIVITY	TEMPERATURE (KELVIN)	QNETPP (W/SQ.M)	RADIOSITY (W/SQ.M)	IRRADIATION (W/SQ.M)
1	0.22000	1800.00	1.1506E+05	1.8694E+05	7.1880E+04
2	0.50000	1047.49	-1.1565E+04	7.9816E+04	9.1382E+04
3	0.17000	1047.92	1.1544E+04	1.2003E+04	4.5919E+02
4	1.00000	300.00	0.0000E+00	4.5919E+02	4.5919E+02



## APPENDIX B - COMPUTER PROGRAM LISTING

```

C
C PROGRAM TO DETERMINE THE SIZE OF A MAIN RADIATOR AND
C A SECONDARY RADIATOR ALONG WITH THE MAXIMUM OPERATING
C TEMPERATURES OF THE PCU AND PAYLOAD
C
C WRITTEN BY DEAN DOBRANICH, NOV. 1986
C
C INPUT: UNIT 5
C OUTPUT: UNIT 6 (MAIN), UNIT 7 (VIEW FACTORS), UNIT 8 (ITERATIONS)
C
COMMON/X/XPCU,XCPL
COMMON/EMIS/EMIS(100)
COMMON/HT/ONETPP(100),T(100),R(100),G(100)
COMMON/OUT/PMR,PSR,PPCUS,PCU,PPLS,PPL,PCUWH,PLWH,REFPOWE,
1 PSR1,PSR2,AREAMR,AREASR,TAVGPCUS,TAVGPLS,COP,
2 TISSR,TOSMR,TISSR,TOSSR,HAPCU,HAPL,CPCU,CPL,
3 THPOWER,THPNEW
COMMON/DIMS/DPCUS,HPCUS,DPCU,HPCU,DPLS,HPLS,DPL,HPL,
1 SD1,SD2,SD3
COMMON/AREA/APCUSL,APCUSC,APCUSR,APCUL,APCUC,APCUR,
1 APLSL,APLSC,APLSR,APLL,APLC,APLR,
2 APL,APCU,APLS,APCUS
C
DIMENSION IDSURF(100),IDCON(100),IST(20)
DIMENSION TSMR(50),TSSR(50),TNODEMR(50),TNODESR(50)
DIMENSION RADMR(50),RADSR(50),POAMR(50),POASR(50),AMR(50),ASR(50)
DIMENSION RNODEMR(50),RNODESR(50)
C
DIMENSION TPCU(4),TPL(4),RPCU(4),RPL(4),FPCU(4,4),FPL(4,4)
DIMENSION ECPCU(4),ECPL(4)
C
PI=3.141592654
C
READ(5,*)NOUTERMAX
READ(5,*)CONVOUT
READ(5,*)NRHMAX
READ(5,*)CONVRH
C
READ(5,*)NMR
READ(5,*)NSR
C
READ(5,*)EMR1
READ(5,*)EMR2
READ(5,*)ESR1
READ(5,*)ESR2
READ(5,*)EPCUS1L,EPCUS1C,EPCUS1R
READ(5,*)EPCUS2L,EPCUS2C,EPCUS2R
READ(5,*)EPLS1L,EPLS1C,EPLS1R
READ(5,*)EPLS2L,EPLS2C,EPLS2R
READ(5,*)EPCU
READ(5,*)EPL
C
READ(5,*)TSPACE
C
READ(5,*)TISMR
READ(5,*)TOSMR
READ(5,*)TISSR
READ(5,*)TOSSR
C
READ(5,*)RADMR1
READ(5,*)RADSR1
READ(5,*)SD1
READ(5,*)SD2
READ(5,*)SD3
C
READ(5,*)DPCUS
READ(5,*)HPCUS
READ(5,*)DPLS
READ(5,*)HPLS
READ(5,*)DPCU
READ(5,*)HPCU
READ(5,*)DPL
READ(5,*)HPL
C
READ(5,*)THPOWER
READ(5,*)EFFIC
READ(5,*)FCCOP
C
READ(5,*)FEPPCU
READ(5,*)FPCUWHAC
READ(5,*)FEPLL
READ(5,*)FPLWHAC
C
READ(5,*)DELTSR
READ(5,*)CPCU
READ(5,*)CPL
C
IDEBUG=0
IF(NOUTERMAX.LT.0)IDEBUG=1
NOUTERMAX=ABS(NOUTERMAX)
NCV=2
IDROPSP=ABS(TISSR-TOSSR)
IF(DELTSR.LT.0)NCV=0
IF(RADMR1.LE.DPCUS*0.5)RADMR1=1.01*DPCUS*0.5
IF(RADSR1.LE.DPLS*0.5)RADSR1=1.01*DPLS*0.5
C IF REFRIGERATOR USED TO COOL PAYLOAD, NO ACTIVE COOLING OF PCU ALLOWED
IF(FCCOP.NE.0.0)FPCUWHAC=0.0
COP=0.0
THPNEW=0.0
REFPOWE=0.0
C
C COMPONENT POWERS (BEFORE ADJUSTMENT FOR CONDUCTION AND CONVECTION)
ELECPOW=THPOWER*EFFIC
PMR=THPOWER-ELECPOW

```

```

PCUWH=FEPPCU*ELECPOW
PSR1=FPCUWHAC*PCUWH
PPCUS=0.0
PPCU=PCUWH-PSR1-PPCUS
PLWH=FEPL*(ELECPOW-PCUWH)
PSR2=FPLWHAC*PLWH
PPLS=0.0
PPL=PLWH-PSR2-PPLS
PSR=PSR1+PSR2

C
C COMPONENT AREAS
APCUSC=P1*DPCUS*HPCUS
APLSC=P1*DPLS*HPLS
APCUSL=P1*DPCUS*DPCUS*0.25
APLSL=P1*DPLS*DPLS*0.25
APCUSR=APCUSL
APLSR=APLSL
APCUC=P1*DPCU*HPCU
APLC=P1*DPL*HPL
APCUL=P1*DPCU*DPCU*0.25
APLL=P1*DPL*DPL*0.25
APCUR=APCUL
APLR=APLL

C
APCUS=APCUSC+APCUSL+APCUSR
APLS=APLSC+APLSL+APLSR
APCU=APCUC+APCUL+APCUR
APL=APLC+APLL+APLR

C
C SET UP POINTERS
IST(1)=1
IST(2)=IST(1)+NMR
IST(3)=IST(2)+NMR
IST(4)=IST(3)+NSR
IST(5)=IST(4)+NSR
IST(6)=IST(5)+1
IST(7)=IST(6)+1
IST(8)=IST(7)+1
IST(9)=IST(8)+1
IST(10)=IST(9)+1
IST(11)=IST(10)+1
IST(12)=IST(11)+1
IST(13)=IST(12)+1
IST(14)=IST(13)+1
IST(15)=IST(14)+1
IST(16)=IST(15)+1
IST(17)=IST(16)+1
IST(18)=IST(17)+1
IST(19)=IST(18)+1

C TOTAL NUMBER OF SURFACES
NS=IST(19)

C

C SET EMIS, IDSURF, AND IDCON ARRAYS
C
DO 5 K=1,NS
R(K)=1.0
5 IDCON(K)=0

C
C MAIN RADIATOR
KK=IST(2)
DO 10 K=IST(1),IST(2)-1
EMIS(K)=EMR1
EMIS(KK)=EMR2
IDSURF(K)=0
IDSURF(KK)=0
IDCON(K)=KK
IDCON(KK)=-K
KK=KK+1
10 CONTINUE

C
C SECONDARY RADIATOR
KK=IST(4)
DO 15 K=IST(3),IST(4)-1
EMIS(K)=ESR1
EMIS(KK)=ESR2
IDSURF(K)=0
IDSURF(KK)=0
IDCON(K)=KK
IDCON(KK)=-K
KK=KK+1
15 CONTINUE

C
C PCU SHELL LEFT END
KK=IST(6)
DO 20 K=IST(5),IST(6)-1
EMIS(K)=EPCUS1L
EMIS(KK)=EPCUS2L
IDSURF(K)=2
IDSURF(KK)=2
IDCON(K)=KK
IDCON(KK)=-K
ONETPP(K)=PPCUS/APCUSL/2.0
ONETPP(KK)=ONETPP(K)
KK=KK+1
20 CONTINUE

C
C PCU SHELL CURVED SURFACE
KK=IST(8)
DO 25 K=IST(7),IST(8)-1
EMIS(K)=EPCUS1C
EMIS(KK)=EPCUS2C
IDSURF(K)=2
IDSURF(KK)=2
IDCON(K)=KK

```

```

      IDCON(KK)=-K
      ONETPP(K)=PPCUS/APCUSC/2.0
      ONETPP(KK)=ONETPP(K)
      KK=KK+1
25  CONTINUE
C
C   PCU SHELL RIGHT END
      KK=IST(10)
      DO 30 K=IST(9),IST(10)-1
      EMIS(K)=EPCUS1R
      EMIS(KK)=EPCUS2R
      IDSURF(K)=2
      IDSURF(KK)=2
      IDCON(K)=KK
      IDCON(KK)=-K
      ONETPP(K)=PPCUS/APCUSR/2.0
      ONETPP(KK)=ONETPP(K)
      KK=KK+1
30  CONTINUE
C
C   PAYLOAD SHELL LEFT END
      KK=IST(12)
      DO 35 K=IST(11),IST(12)-1
      EMIS(K)=EPLS1L
      EMIS(KK)=EPCUS2L
      IDSURF(K)=2
      IDSURF(KK)=2
      IDCON(K)=KK
      IDCON(KK)=-K
      ONETPP(K)=PPLS/APLSL/2.0
      ONETPP(KK)=ONETPP(K)
      KK=KK+1
35  CONTINUE
C
C   PAYLOAD SHELL CURVED SURFACE
      KK=IST(14)
      DO 40 K=IST(13),IST(14)-1
      EMIS(K)=EPLS1C
      EMIS(KK)=EPCUS2C
      IDSURF(K)=2
      IDSURF(KK)=2
      IDCON(K)=KK
      IDCON(KK)=-K
      ONETPP(K)=PPLS/APLSC/2.0
      ONETPP(KK)=ONETPP(K)
      KK=KK+1
40  CONTINUE
C
C   PAYLOAD SHELL RIGHT END
      KK=IST(16)
      DO 45 K=IST(15),IST(16)-1
      EMIS(K)=EPLS1R

      EMIS(KK)=EPCUS2R
      IDSURF(K)=2
      IDSURF(KK)=2
      IDCON(K)=KK
      IDCON(KK)=-K
      ONETPP(K)=PPLS/APLSR/2.0
      ONETPP(KK)=ONETPP(K)
      KK=KK+1
45  CONTINUE
C
C   PCU
      EMIS(IST(17))=EPCU
      IDSURF(IST(17))=1
      ONETPP(IST(17))=PPCU/APCU
C
C   PAYLOAD
      EMIS(IST(18))=EPL
      IDSURF(IST(18))=1
      ONETPP(IST(18))=PPL/APL
C
C   SPACE
      EMIS(IST(19))=1.0
      IDSURF(IST(19))=0
      T(IST(19))=TSPACE
C
C   INITIAL GUESS FOR EFFECTIVE TEMPERATURES
      DO 60 J=1,NMR
60   TSMR(J)=TSPACE
      DO 65 J=1,NSR
65   TSSR(J)=TSPACE
C
C   RADMR(1)=RADMR1
      RADSR(1)=RADSR1
      PNMR=PMR/NMR
      PNSR=PSR/NSR
      EAVGMR=(EMR1+EMR2)/2.0
      EAVGSR=(ESR1+ESR2)/2.0
C   WRITE SURFACE ID ARRAYS
      CALL IDOUT(NS,NMR,NSR,IDSURF,IDCON)
C   DETERMINE VIEW FACTORS FOR SURFACES NOT DEPENDENT ON
C   THE SIZE OF THE MAIN AND SECONDARY RADIATORS
      CALL VIEW1(NS,IST)
C   SET UP ARRAYS FOR SOLVING COMBINED RADIATION/CONDUCTION
      DO 120 I=1,4
      RPCI(I)=1.0
      RPL(I)=1.0
120  ECPCU(1)=EPCUS1L
      ECPCU(2)=EPCUS1C
      ECPCU(3)=EPCUS1R
      ECPCU(4)=EPCU
      ECPL(1)=EPLS1L
      ECPL(2)=EPLS1C

```

```

ECPL(3)=EPLS1R
ECPL(4)=EPL
CALL FASSIGN(0,IST,FPCU)
CALL FASSIGN(1,IST,FPL)
C
C *****
C
DO 600 ICV=1,NCV+1
DO 500 IOUTER=1,NO OUTERMAX
C
C FIRST ESTIMATE THE SIZE OF THE MAIN RADIATOR
CALL RADSIZE(NMR,PMR,TISMR,TOSMR,EAVGMR,TSMR,RADMR,AMR,
1 TNODEMR,RNODEMR)
C ASSIGN TNODEMR ARRAY TO T ARRAY
KK=IST(2)
K=1
DO 75 J=IST(1),IST(2)-1
T(J)=TNODEMR(K)
T(KK)=TNODEMR(K)
K=K+1
KK=KK+1
75 CONTINUE
C
C NOW ESTIMATE SIZE OF THE SECONDARY RADIATOR
CALL RADSIZE(NSR,PSR,TISSR,TOSSR,EAVGSR,TSSR,RADSR,ASR,
1 TNODESR,RNODESR)
C ASSIGN TNODESR ARRAY TO T ARRAY
KK=IST(4)
K=1
DO 80 J=IST(3),IST(4)-1
T(J)=TNODESR(K)
T(KK)=TNODESR(K)
K=K+1
KK=KK+1
80 CONTINUE
C
C NOW DETERMINE VIEW FACTORS FOR ALL SURFACES BASED ON ESTIMATED
C AREAS. THEN, SOLVE FOR RADIOSITIES, ONETPP'S, AND T'S.
C
CALL VIEW2(NS,NMR,NSR,IST,RADMR,AMR,RADSR,ASR)
NITER=NRHMAX
CALL RADHT(NS,IDSURF,IDCON,CONVRH,NITER)
C
C DETERMINE POA BASED ON CALCULATED ONETPP'S OF MAIN AND SECONDARY RADIATORS
C WHERE: POA = ONETPP(SIDE 1) + ONETPP(SIDE 2)
C ALSO, CHECK FOR CONVERGENCE OF ONETPP'S
C
C MAIN RADIATOR FIRST
RELERRM=0.0
POWTOTMR=0.0
KK=IST(2)
K=1
DO 100 J=IST(1),IST(2)-1
POAMR(K)=ONETPP(J)+ONETPP(KK)
PNMRNEW=POAMR(K)*AMR(K)
POWTOTMR=POWTOTMR+PNMRNEW
RELERR=ABS(PNMR-PNMRNEW)/PNMR
RELERRM=AMAX1(RELERR,RELERRM)
K=K+1
KK=KK+1
100 CONTINUE
C
C SECONDARY RADIATOR LAST
POWTOTSR=0.0
KK=IST(4)
K=1
DO 105 J=IST(3),IST(4)-1
POASR(K)=ONETPP(J)+ONETPP(KK)
PNSRNEW=POASR(K)*ASR(K)
POWTOTSR=POWTOTSR+PNSRNEW
RELERR=ABS(PNSR-PNSRNEW)/PNSR
RELERRM=AMAX1(RELERR,RELERRM)
K=K+1
KK=KK+1
105 CONTINUE
C
WRITE(8,88)IOUTER,NITER,RELERRM,POWTOTMR,POWTOTSR
88 FORMAT(' ',/,4X,12.3X,12.3X,1PE12.4,3X,E12.4,3X,E12.4)
IF(RELERRM.LT.CONVOUT)GO TO 505
C
IF(IDEBUG.EQ.1.AND.ICV.GT.NCV)THEN
CALL FOUT(NS)
CALL ROUT(NMR,NSR,TNODEMR,TNODESR,TSMR,TSSR,
1 POAMR,POASR,RADMR,RADSR,AMR,ASR,RNODEMR,RNODESR)
CALL OUT1(NS)
ELSE
ENDIF
C
C CALCULATE NEW EFFECTIVE TEMPERATURES (TSNEW'S) IF CONVERGENCE NOT MET
CALL TSNEW(NMR,EAVGMR,TNODEMR,POAMR,TSMR)
CALL TSNEW(NSR,EAVGSR,TNODESR,POASR,TSSR)
C AND REPEAT THE ENTIRE PROCESS...
C
500 CONTINUE
WRITE(6,499)
499 FORMAT(' ',/,4X,'-*** WARNING - OUTER ITERATION DID
1 NOT CONVERGE ***-'./)
C
C *****
C
505 CONTINUE
C
AREAMR=P1*(RADMR(NMR+1)**2-RADMR1**2)
AREASR=P1*(RADSR(NSR+1)**2-RADSR1**2)

```

```

C NOW ACCOUNT FOR CONDUCTION BETWEEN PCU AND PCU SHELL
C
C USE AVERAGE TEMPERATURE OF SHELL TO ALLOW FOR MAXIMUM POSSIBLE
C TEMPERATURE REDUCTION DUE TO CONDUCTION
TAVGPCUS=(T(IST(5))*APCUSL+T(IST(7))*APCUS+
1 T(IST(9))*APCUSR)/APCUS
TAVGPLS=(T(IST(11))*APLSL+T(IST(13))*APLSC+
1 T(IST(15))*APLSR)/APLS
TPCU(1)=TAVGPCUS
TPCU(2)=TAVGPCUS
TPCU(3)=TAVGPCUS
TPL(1)=TAVGPLS
TPL(2)=TAVGPLS
TPL(3)=TAVGPLS
C
C WRITE FINAL OUTPUT FOR NO-SHELL CONDUCTION CASE
C CALL OUT2(IST)
C
C USING MODIFIED REGULA FALSI METHOD TO FIND ROOT OF FUNCTION FUN
C SUCH THAT FUN(ROOT)=WASTE HEAT-RADIATED HEAT-CONDUCTED HEAT=0
C FIRST PCU (H1 AND H2 PROVIDE AN INTERVAL CONTAINING A ROOT)
IF(CPCU.LE.0.0)GO TO 150
H1=0.0
H2=PPCU
ROOTN=PPCU
XC=0.0
CALL FUN(PPCU,APCU,ECPCU,RPCU,FPCU,TPCU,CPCU,XC,H1,FH)
CALL FUN(PPCU,APCU,ECPCU,RPCU,FPCU,TPCU,CPCU,XC,H2,GH)
ROOTO=H2
DO 125 IM=1,20
GMF=GH-FH
IF(ABS(GMF).LT.1.0E-15)GO TO 150
ROOTN=(GH+H1-FH*H2)/GMF
C CHECK FOR ERROR
IF(ABS((ROOTN-ROOTO)/ROOTN).GT.0.002)GO TO 140
CALL FUN(PPCU,APCU,ECPCU,RPCU,FPCU,TPCU,CPCU,XC,ROOTN,FROOT)
GO TO 150
140 CALL FUN(PPCU,APCU,ECPCU,RPCU,FPCU,TPCU,CPCU,XC,ROOTN,FROOT)
IF(FH+FROOT.GT.0.0)GO TO 130
H2=ROOTN
GH=FROOT
FH=0.5*FH
GO TO 135
130 H1=ROOTN
FH=FROOT
GH=0.5*GH
135 CONTINUE
ROOTO=ROOTN
125 CONTINUE
GO TO 170
C
150 CONTINUE
IF(CPCU.EQ.0.0)GO TO 175
TPCU(4)=AMAX1(TPCU(1),TPCU(2),TPCU(3))-CPCU
CALL FUN(PPCU,APCU,ECPCU,RPCU,FPCU,TPCU,CPCU,XCPCU,ROOTN,FROOT)
170 PPCU=ROOTN
PPCUS=PCUWH-PSR1-PPCU
ONETPP(IST(17))=PPCU/APCU
ONETPP(IST(5))=PPCUS/APCUS
ONETPP(IST(7))=PPCUS/APCUS
ONETPP(IST(9))=PPCUS/APCUS
ONETPP(IST(6))=0.0
ONETPP(IST(8))=0.0
ONETPP(IST(10))=0.0
175 CONTINUE
C
C REPEAT FOR PAYLOAD
IF(CPL.LE.0.0)GO TO 250
H1=0.0
H2=PPL
ROOTN=PPL
XC=0.0
CALL FUN(PPL,APL,ECPL,RPL,FPL,TPL,CPL,XC,H1,FH)
CALL FUN(PPL,APL,ECPL,RPL,FPL,TPL,CPL,XC,H2,GH)
ROOTO=H2
DO 225 IM=1,20
GMF=GH-FH
IF(ABS(GMF).LT.1.0E-15)GO TO 250
ROOTN=(GH+H1-FH*H2)/GMF
C CHECK FOR ERROR
IF(ABS((ROOTN-ROOTO)/ROOTN).GT.0.002)GO TO 240
CALL FUN(PPL,APL,ECPL,RPL,FPL,TPL,CPL,XC,ROOTN,FROOT)
GO TO 250
240 CALL FUN(PPL,APL,ECPL,RPL,FPL,TPL,CPL,XC,ROOTN,FROOT)
IF(FH+FROOT.GT.0.0)GO TO 230
H2=ROOTN
GH=FROOT
FH=0.5*FH
GO TO 235
230 H1=ROOTN
FH=FROOT
GH=0.5*GH
235 CONTINUE
ROOTO=ROOTN
225 CONTINUE
GO TO 270
C
250 CONTINUE
IF(CPL.EQ.0.0)GO TO 275
TPL(4)=AMAX1(TPL(1),TPL(2),TPL(3))-CPL
CALL FUN(PPL,APL,ECPL,RPL,FPL,TPL,CPL,XCPL,ROOTN,FROOT)
270 PPCU=ROOTN
PPL=ROOTN

```

```

PPLS=PLWH-PSR2-PPL
ONETPP(IST(18))=PPL/APL
ONETPP(IST(11))=PPL/APLS
ONETPP(IST(13))=PPL/APLS
ONETPP(IST(15))=PPL/APLS
ONETPP(IST(12))=0.0
ONETPP(IST(14))=0.0
ONETPP(IST(16))=0.0
275 CONTINUE
C
C RE-SOLVE RADIATION HEAT TRANSFER FOR ENTIRE PLATFORM USING
C PCU AND PL WASTE HEAT VALUES CORRECTED FOR CONDUCTION TO SHELL
C
NITER=NRHMAX
CALL RADHT(NS,IDSURF,IDCON,CONVRH,NITER)
C
TAVGPCUS=(T(IST(5))*APCUSL+T(IST(7))*APCUSC+
1 T(IST(9))*APCUSR)/APCUS
TAVGPLS=(T(IST(11))*APLSL+T(IST(13))*APLSC+
1 T(IST(15))*APLSR)/APLS
C
C ADJUST MAX SEC RADIATOR TEMP SO THAT IT DOES NOT EXCEED MAX OF
C PL OR PCU TEMPS (OTHERWISE, A REFRIGERATION UNIT WOULD BE NEEDED)
IF(NCV.EQ.0.OR.FCCOP.NE.0.0)GO TO 599
TM1=T(IST(17))
IF(PSR1.LT.1.0)TM1=0.0
TM2=T(IST(18))
IF(PSR2.LT.1.0)TM2=0.0
IF(TISSR.GT.TOSSR)THEN
TISSR=AMAX1(TM1,TM2)-DELTSR*0.97
TOSSR=TISSR-TDROPSR
ELSE
TOSSR=AMAX1(TM1,TM2)-DELTSR*0.97
TISSR=TOSSR-TDROPSR
ENDIF
C CALCULATE REQUIRED HA FOR CONVECTION COOLING OF PCU AND PL
C (IF HA IS NEGATIVE, A REFRIGERATION UNIT IS REQUIRED)
599 TCAVG=(TISSR+TOSSR)/2.0
HAPCU=PSR1/(T(IST(17))-TCAVG)
HAPL=PSR2/(T(IST(18))-TCAVG)
C IF A REFRIGERATOR IS USED TO COOL PAYLOAD:
IF(FCCOP.EQ.0.0.OR.ICV.GT.NCV)GO TO 600
COP=FCCOP*(1.0/(TISSR/(T(IST(18))-0.96*DELTSR))-1.0)
REFPOWE=PSR2/COP
REFPOWT=REFPOWE/EFFIC
THPNEW=THPOWER+REFPOWT
ELECPOW=THPNEW*EFFIC
PMR=THPNEW-ELECPOW
PNMR=PMR/NMR
PSR1=0.0
PPCUS=0.0
PCUWH=FEPPCU+ELECPOW

PPCU=PCUWH
ONETPP(IST(17))=PPCU/APCU
ONETPP(IST(5))=PPCUS/APCUS
ONETPP(IST(7))=PPCUS/APCUS
ONETPP(IST(9))=PPCUS/APCUS
ONETPP(IST(6))=0.0
ONETPP(IST(8))=0.0
ONETPP(IST(10))=0.0
600 CONTINUE
C
C NOW WRITE ALL FINAL OUTPUT
CALL FOUT(NS)
CALL ROUT(NMR,NSR,TNODEMR,TNODESR,TSMR,TSSR,
1 POAMR,POASR,RADMR,RADSR,AMR,ASR,RNODEMR,RNODESR)
CALL OUT1(NS)
CALL OUT2(IST)
C
STOP
END
C
C -----SUBROUTINES-----
C
SUBROUTINE RADSIZE(NN,P,TIS,TOS,EAVG,TS,RAD,A,TNODE,RNODE)
C THIS SUBROUTINE DETERMINES THE REQUIRED SIZE OF THE RADIATOR NODES
C BASED ON AN ESTIMATED EFFECTIVE BACKGROUND TEMPERATURE (TS).
C
DIMENSION RAD(NN+1),TS(NN),TNODE(NN),RNODE(NN),A(NN)
C
P1=3.141592654
C
IF(ABS(TIS-TOS).GT.2.0)THEN
FOR A BRAYTON CYCLE:
C
C2=-1.0/4.0/P1/SIGMA/EAVG
C2=-1.48373E06/EAVG
C1=C2*P/ABS(TIS-TOS)
C LET EACH NODE HAVE THE SAME TEMPERATURE DROP; DETERMINE
C NODE RADII SUCH THAT POWER DEPOSITED IN NODE EQUALS POWER
C REMOVED FROM BOTH SIDES OF NODE VIA RADIATION
DT=(TOS-TIS)/NN
C FOR OUTSIDE-IN FLOW
SIGN=1.0
C FOR INSIDE-OUT FLOW
IF(DT.LT.0.0)SIGN=-1.0
DO 5 I=1,NN
T0=TIS+DT*(I-1)
T1=TIS+DT*I
ARG=AMIN1(T0,T1)
C TS CAN NOT BE GREATER THAN ARG
IF(TS(I).GE.ARG)TS(I)=ARG*0.998
TRATIO=(TS(I)+T1)/(TS(I)-T1)*(TS(I)-T0)/(TS(I)+T0)
RAD(I+1)=(RAD(I)**2+SIGN*C1*0.5/TS(I))*3*

```

```

1      (ALOG(TRATIO)+2.0*ATAN(T1/TS(1))-
2      2.0*ATAN(T0/TS(1)))*.5
C
C 5 CONTINUE
C
C DETERMINE AVERAGE NODE TEMPERATURE BASED ON TEMPERATURES AT END
C OF EACH NODE AND THE NODE EFFECTIVE BACKGROUND TEMPERATURE;
C ALSO, CALCULATE R AT WHICH AVERAGE TEMPERATURE OCCURS
C
C3=C1*PI
ADT=ABS(DT)
DO 10 I=1,NN
A(I)=PI*(RAD(I+1)**2-RAD(I)**2)
TNODE(I)=(TS(I)**4-2.0*C3*ADT/A(I))*.25
T0=TIS+DT*(I-1)
T1=TNODE(I)
TRATIO=(TS(I)+T1)/(TS(I)-T1)*(TS(I)-T0)/(TS(I)+T0)
RNODE(I)=(RAD(I)**2+SIGN(C1*.5/TS(I))*.3*
1      (ALOG(TRATIO)+2.0*ATAN(T1/TS(1))-
2      2.0*ATAN(T0/TS(1)))*.5
10 CONTINUE
C
C RETURN
C
C ELSE
C FOR A RANKINE CYCLE:
C
PONN=P/NN
TIS4=TIS**.4
C4=2.0*5.669E-8*EAVG
DO 15 I=1,NN
A(I)=PONN/C4/(TIS4-TS(I)**4)
RAD(I+1)=(A(I)/PI+RAD(I)**2)*.0.5
RNODE(I)=0.5*(RAD(I)+RAD(I+1))
TNODE(I)=TIS
15 CONTINUE
C
C ENDIF
C RETURN
C
C END
C
C ---*---
C
SUBROUTINE TSNEW(NN,EAVG,TNODE,POA,TS)
C THIS SUBROUTINE FINDS NEW EFFECTIVE BACKGROUND TEMPERATURES
C DIMENSION TNODE(NN),POA(NN),TS(NN)
C
C1=1/2/SIGMA/EAVG
C1=8.820E06/EAVG
C WEIGHTING FACTOR USED TO DAMPEN OSCILLATIONS AND SPEED CONVERGENCE
WF=0.8
C
DO 5 I=1,NN
TS(I)=WF*(TNODE(I)**4-POA(I)*C1)**.25+(1.0-WF)*TS(I)
5 CONTINUE
C
C RETURN
C
C END
C
C ---*---
C
SUBROUTINE RADHT(N,IDSURF,IDCON,CONV,NITER)
COMMON/CVIEW/F(100,100)
COMMON/EMIS/EMIS(100)
COMMON/HT/ONETPP(100),T(100),R(100),G(100)
DIMENSION V(100),IDSURF(N),IDCON(N)
C
C CALCULATE RADIOSITIES, IRRADIATIONS, AND HEAT FLUXES
C USING NETWORK METHOD FOR RADIATION HEAT TRANSFER
C (REF. HOLMAN, HEAT TRANSFER)
C
C -----
C IDSURF = 0 FOR SURFACES WITH KNOWN TEMPERATURE
C IDSURF = 1 FOR SURFACES WITH KNOWN HEAT FLUX
C IDSURF = 2 FOR TWO-SIDED SURFACES WITH T1=T2, QT=Q1+Q2
C -----
C IDCON ARRAY DEFINES WHICH TWO-SIDED SURFACES ARE CONNECTED;
C SIDE 2 OF A CONNECTION MUST BE INDICATED AS A NEGATIVE.
C EXAMPLE: IF SURFACE 5 AND 22 ARE CONNECTED -
C IDCON(5)=22 SIDE 1
C IDCON(22)=-5 SIDE 2
C
C SIGMA=5.669E-8
C
C USING GAUSS-SEIDEL TO SOLVE NXN EQUATIONS
C INITIAL GUESS FOR RADIOSITIES
C DO 51 I=1,N
51 V(I)=R(I)
C
C DO 99 IT=1,NITER
C CALCULATE R FOR SURFACES WITH KNOWN TEMPERATURE
C DO 61 I=1,N
C IF (IDSURF(I).NE.0)GO TO 61
C X=1.0-EMIS(I)
C XX=1.0-F(I,I)*X
C SUM=0.0
C DO 71 J=1,N
C IF (J.EQ.I)GO TO 71
C SUM=SUM+F(I,J)*R(J)
71 CONTINUE
C R(I)=(X*SUM+EMIS(I)*SIGMA*T(I)**4.0)/XX
61 CONTINUE
C
C CALCULATE R FOR SURFACES WITH KNOWN HEAT FLUX

```

```

DO 62 I=1,N
IF(1DSURF(I).NE.1)GO TO 62
Y=1.0/(1.0-F(I,I))
SUM=0.0
DO 65 J=1,N
IF(J.EQ.1)GO TO 65
SUM=SUM+F(I,J)*R(J)
65 CONTINUE
R(I)=Y*(SUM+ONETPP(I))
62 CONTINUE
C
C CALCULATE R FOR SURFACES THAT ARE OPPOSITE SIDES OF THE SAME
C STRUCTURE SUCH THAT Q(TOTAL) = Q(I) + Q(K) AND T(I) = T(K).
C K = 1DCON(I) DEFINES SURFACE CONNECTIONS
C
DO 63 I=1,N
IF(1DSURF(I).NE.2)GO TO 63
C
K=1DCON(I)
IF(K.LE.0)GO TO 63
X1=1.0/EMIS(I)
A1=1.0/(X1-F(I,I)*(X1-1.0))
B1=1.0/(1.0-F(K,K))
X2=1.0/EMIS(K)
A2=1.0/(X2-F(K,K)*(X2-1.0))
B2=1.0/(1.0-F(I,I))
SUM1=0.0
SUM2=0.0
DO 10 J=1,N
IF(J.EQ.1)GO TO 10
SUM1=SUM1+F(I,J)*R(J)
SUM2=SUM2+F(K,J)*R(J)
10 CONTINUE
SUM3=0.0
DO 12 J=1,N
IF(J.EQ.K)GO TO 12
SUM3=SUM3+(F(I,J)+F(K,J))*R(J)
12 CONTINUE
R(I)=A1*((X1-1.0)*SUM1-(X2-1.0)*SUM2+B1*X2*(ONETPP(I)+
1 ONETPP(K)+SUM3))/(1.0+A1*B1*X2)
C
SUM1=0.0
SUM2=0.0
DO 15 J=1,N
IF(J.EQ.K)GO TO 15
SUM1=SUM1+F(K,J)*R(J)
SUM2=SUM2+F(I,J)*R(J)
15 CONTINUE
SUM3=0.0
DO 17 J=1,N
IF(J.EQ.1)GO TO 17
SUM3=SUM3+(F(I,J)+F(K,J))*R(J)
17 CONTINUE
R(K)=A2*((X2-1.0)*SUM1-(X1-1.0)*SUM2+B2*X1*(ONETPP(I)+
1 ONETPP(K)+SUM3))/(1.0+A2*B2*X1)
C
63 CONTINUE
C
C CHECK FOR CONVERGENCE
C
DIFF=0.0
DO 81 I=1,N
DN=0.0
IF(ABS(V(I)).GT.0.0)DN=ABS((R(I)-V(I))/V(I))
81 DIFF=AMAX1(DIFF,DN)
IF(DIFF.LT.CONV.AND.DIFF.NE.0.0)GO TO 101
DO 82 I=1,N
82 V(I)=R(I)
99 CONTINUE
101 CONTINUE
C
C-----
C DETERMINE IRRADIATIONS G, FOR EACH SURFACE
DO 120 I=1,N
SUM=0.0
DO 110 K=1,N
110 SUM=SUM+F(I,K)*R(K)
120 G(I)=SUM
C
C DETERMINE ONETPP AND T FOR EACH SURFACE (WATTS/M**2. AND K)
C
DO 125 I=1,N
IF(1DSURF(I).NE.1)ONETPP(I)=R(I)-G(I)
IF(1DSURF(I).NE.0)THEN
XX=0.0
IF(EMIS(I).NE.0.0)XX=(1.0-EMIS(I))/EMIS(I)*ONETPP(I)/SIGMA
T(I)=(XX+R(I)/SIGMA)*0.25
ELSE
ENDIF
125 CONTINUE
C
NITER=IT
RETURN
END
C
C-----
C
SUBROUTINE FUN(WH,A,EMIS,R,F,T,C,XC,Q,FV)
FUN = WASTE HEAT - HEAT RADIATED - HEAT CONDUCTED
USED TO COUPLE RADIATION AND CONDUCTION HEAT TRANSFER
C
DIMENSION EMIS(4),R(4),ONETPP(4),F(4,4),T(4)
DIMENSION G(4),V(4)

```



```

C INITIALIZE ALL F'S TO 0.0
DO 5 L=1,N
DO 10 M=1,N
10 F(L,M)=0.0
5 CONTINUE
C
C DETERMINE VIEW FACTOR BETWEEN PCUSR AND PLSL
F(IST(10),IST(12))=DTOD(0.5*DPCUS,0.5*DPLS,SD1+SD2+SD3)
F(IST(12),IST(10))=F(IST(10),IST(12))*APCUSR/APLSL
C
C DETERMINE VIEW FACTORS BETWEEN PCU AND PCU SHELL SURFACES
15=IST(5)
17=IST(7)
19=IST(9)
117=IST(17)
SD=(HPCUS-HPCU)*0.5
FA=DTOD(0.5*DPCU,0.5*DPCUS,SD)
CALL CTORING(0.5*DPCU,HPCU,0.5*DPCU,0.5*DPCUS,SD,FB)
FB=AMAX1(0.0,FB)
F(117,15)=APCUL/APCU*FA+APCUC/APCU*FB
F(117,19)=F(117,15)
F(117,17)=2.0*APCUL/APCU*(1.0-FA)+APCUC/APCU*(1.0-2.0*FB)
F(15,117)=APCU/APCUSL*F(117,15)
F(19,117)=F(15,117)
F(17,117)=APCU/APCUC*F(117,17)
C ACCOUNT FOR PCU BLOCKAGE
B=(DPCUS-DPCU)*0.5
D=B*(HPCUS/(HPCU+SD))-1.0)
D=AMIN1(D,0.5*DPCU)
DP=D+B
CALL FRINGS(0.5*DPCUS-DP,0.5*DPCUS,0.5*DPCU,0.5*DPCUS,
1 HPCUS,F(15,19))
F(19,15)=F(15,19)
F(15,17)=1.0-F(15,117)-F(15,19)
F(19,17)=F(15,17)
F(17,15)=APCUSL/APCUC*F(15,17)
F(17,19)=F(17,15)
F(17,17)=1.0-2.0*F(17,15)-F(17,117)
C
C DETERMINE VIEW FACTORS BETWEEN PL AND PL SHELL SURFACES
15=IST(5+6)
17=IST(7+6)
19=IST(9+6)
117=IST(17+1)
SD=(HPLS-HPL)*0.5
FA=DTOD(0.5*DPL,0.5*DPLS,SD)
CALL CTORING(0.5*DPL,HPL,0.5*DPL,0.5*DPLS,SD,FB)
FB=AMAX1(0.0,FB)
F(117,15)=APLL/APL*FA+APLC/APL*FB
F(117,19)=F(117,15)
F(117,17)=2.0*APLL/APL*(1.0-FA)+APLC/APL*(1.0-2.0*FB)
F(15,117)=APL/APLSL*F(117,15)
F(19,117)=F(15,117)
F(17,117)=APL/APLSC*F(117,17)
C ACCOUNT FOR PL BLOCKAGE
B=(DPLS-DPL)*0.5
D=B*(HPLS/(HPL+SD))-1.0)
D=AMIN1(D,0.5*DPL)
DP=D+B
CALL FRINGS(0.5*DPLS-DP,0.5*DPLS,0.5*DPL,0.5*DPLS,
1 HPLS,F(15,19))
F(19,15)=F(15,19)
F(15,17)=1.0-F(15,117)-F(15,19)
F(19,17)=F(15,17)
F(17,15)=APLSL/APLSC*F(15,17)
F(17,19)=F(17,15)
F(17,17)=1.0-2.0*F(17,15)-F(17,117)
C
RETURN
END
C
C ----*----
C SUBROUTINE VIEW2(N,NMR,NSR,IST,RM,AM,RS,AS)
C CALCULATE VIEW FACTORS FOR ALL REMAINING SURFACES
DIMENSION IST(20),RM(NMR+1),AM(NMR),RS(NSR+1),AS(NSR)
COMMON/CVIEW/F(100,100)
COMMON/AREA/APCUSL,APCUC,APCUSR,APCUL,APCUC,APCUR,
1 APLSL,APLSC,APLSR,APLL,APLC,APLR,
2 APL,APCU,APLS,APCUS
COMMON/DIMS/DPCUS,HPCUS,DPCU,HPCU,DPLS,HPLS,DPL,HPL,
1 SD1,SD2,SD3
C
PI=3.141592654
C
C DETERMINE VIEW FACTORS BETWEEN MAIN AND SECONDARY RADIATORS
K=IST(2)
DO 15 L=1,NMR
KK=IST(3)
DO 20 M=1,NSR
CALL FRINGS(RM(L),RM(L+1),RS(M),RS(M+1),SD2,FL)
FL=AMAX1(0.0,FL)
F(K,KK)=FL
C RECIPROSCITY
F(KK,K)=FL*AM(L)/AS(M)
20 KK=KK+1
15 K=K+1
C
C DETERMINE VIEW FACTORS BETWEEN RIGHT END OF PCU SHELL AND
C SECONDARY RADIATOR
KK=IST(3)
DO 25 M=1,NSR
CALL FRINGS(0.0,0.5*DPCUS,RS(M),RS(M+1),SD1+SD2,FM)
FM=AMAX1(0.0,FM)

```

```

C IF SD1 IS GREATER THAN ZERO, MUST ACCOUNT FOR BLOCKAGE FROM
C MAIN RADIATOR
  FB=0.0
  IF(SD1.GT.0.0)THEN
    B=SD1/(SD1+SD2)*(RS(M+1)-0.5*DPCUS)+0.5*DPCUS
    IF(B.GT.RM(1))THEN
      CALL FRINGS(0.0,0.5*DPCUS,RM(1),B,SD1,FB)
      FB=AMAX1(0.0,FB)
    ELSE
      ENDF
    ELSE
      ENDF
    ELSE
      ENDF
    F(IST(10),KK)=AMAX1(0.0,FM-FB)
    F(KK,IST(10))=FM*APCUSR/AS(M)
  25 KK=KK+1
C
C DETERMINE VIEW FACTORS BETWEEN LEFT END OF PL SHELL AND
C MAIN RADIATOR
  KK=IST(2)
  DO 35 M=1,NMR
    CALL FRINGS(0.0,0.5*DPLS,RM(M),RM(M+1),SD2+SD3,FM)
    FM=AMAX1(0.0,FM)
C IF SD3 IS GREATER THAN ZERO, MUST ACCOUNT FOR BLOCKAGE FROM
C SECONDARY RADIATOR
  FB=0.0
  IF(SD3.GT.0.0)THEN
    B=SD3/(SD2+SD3)*(RM(M+1)-0.5*DPLS)+0.5*DPLS
    IF(B.GT.RS(1))THEN
      CALL FRINGS(0.0,0.5*DPLS,RS(1),B,SD3,FB)
      FB=AMAX1(0.0,FB)
    ELSE
      ENDF
    ELSE
      ENDF
    ELSE
      ENDF
    F(IST(12),KK)=AMAX1(0.0,FM-FB)
    F(KK,IST(12))=FM*APLSL/AM(M)
  35 KK=KK+1
C
C DETERMINE VIEW FACTORS BETWEEN PCU SHELL CURVED SURFACE
C AND MAIN RADIATOR
  K=IST(1)
  DO 45 L=1,NMR
    CALL CTORING(0.5*DPCUS,HPCUS,RM(L),RM(L+1),SD1,FL)
    FL=AMAX1(0.0,FL)
    F(IST(8),K)=FL
    F(K,IST(8))=FL*APCUSC/AM(L)
  45 K=K+1
C
C DETERMINE VIEW FACTORS BETWEEN PCU SHELL AND SECONDARY RADIATOR
C IF VIEW IS NOT BLOCKED BY MAIN RADIATOR
  RB=(HPCUS+SD1)/(HPCUS+SD1+SD2)
  K=IST(3)

  DO 50 L=1,NSR
    B=RB*RS(L+1)
    IF(B.LT.RM(1))THEN
      CALL CTORING(0.5*DPCUS,HPCUS,RS(L),RS(L+1),SD1+SD2,FL)
      FL=AMAX1(0.0,FL)
      F(IST(8),K)=FL
      F(K,IST(8))=FL*APCUSC/AS(L)
    ELSE
      ENDF
  50 K=K+1
C
C DETERMINE VIEW FACTORS BETWEEN PL SHELL CURVED SURFACE
C AND SECONDARY RADIATOR
  K=IST(4)
  DO 55 L=1,NSR
    CALL CTORING(0.5*DPLS,HPLS,RS(L),RS(L+1),SD3,FL)
    FL=AMAX1(0.0,FL)
    F(IST(14),K)=FL
    F(K,IST(14))=FL*APLSC/AS(L)
  55 K=K+1
C
C DETERMINE VIEW FACTORS BETWEEN PAYLOAD SHELL AND MAIN RADIATOR
C IF VIEW IS NOT BLOCKED BY SECONDARY RADIATOR
  RB=(HPLS+SD3)/(HPLS+SD2+SD3)
  K=IST(2)
  DO 60 L=1,NMR
    B=RB*RM(L+1)
    IF(B.LT.RS(1))THEN
      CALL CTORING(0.5*DPLS,HPLS,RM(L),RM(L+1),SD2+SD3,FL)
      FL=AMAX1(0.0,FL)
      F(IST(14),K)=FL
      F(K,IST(14))=FL*APLSC/AM(L)
    ELSE
      ENDF
  60 K=K+1
C
C IF SD1 GREATER THAN ZERO, DETERMINE VIEW FACTOR BETWEEN
C PCU SHELL (RIGHT END) AND MAIN RADIATOR
  IF(SD1.GT.0.0)THEN
    K=IST(1)
    DO 65 L=1,NMR
      CALL FRINGS(0.0,0.5*DPCUS,RM(L),RM(L+1),SD1,FL)
      FL=AMAX1(0.0,FL)
      F(IST(10),K)=FL
      F(K,IST(10))=FL*APCUSR/AM(L)
  65 K=K+1
    ELSE
      ENDF
C
C IF SD3 GREATER THAN ZERO, DETERMINE VIEW FACTOR BETWEEN
C PAYLOAD SHELL (LEFT END) AND SECONDARY RADIATOR
  IF(SD3.GT.0.0)THEN

```

```

      K=IST(4)
      DO 75 L=1,NSR
      CALL FRINGS(0.0,0.5*DPLS,RS(L),RS(L+1),SD3,FL)
      FL=AMAX1(0.0,FL)
      F(IST(12),K)=FL
      F(K,IST(12))=FL*APLSR/AS(L)
75  K=K+1
      ELSE
      ENDIF

C
C VIEW FACTORS BETWEEN ALL SURFACES AND SPACE
C
C MAIN RADIATOR
      K=IST(2)
      J=IST(1)
      DO 85 L=1,NMR
      SUM=0.0
      KK=IST(3)
      DO 90 M=1,NSR
      SUM=SUM+F(K,KK)
90  KK=KK+1
      SUM=SUM+F(K,IST(12))+F(K,IST(14))
      F(K,IST(19))=1.0-SUM
      F(J,IST(19))=1.0-F(J,IST(10))-F(J,IST(8))
      K=K+1
85  J=J+1
C
C SECONDARY RADIATOR
      K=IST(3)
      J=IST(4)
      DO 95 L=1,NSR
      SUM=0.0
      KK=IST(2)
      DO 100 M=1,NMR
      SUM=SUM+F(K,KK)
100 KK=KK+1
      SUM=SUM+F(K,IST(10))+F(K,IST(8))
      F(K,IST(19))=1.0-SUM
      F(J,IST(19))=1.0-F(J,IST(12))-F(J,IST(14))
      K=K+1
95  J=J+1
C
C PCU SHELL
      F(IST(6),IST(19))=1.0
      J=IST(3)
      SUM1=0.0
      SUM2=0.0
      DO 105 L=1,NSR
      SUM1=SUM1+F(IST(10),J)
      SUM2=SUM2+F(IST(8),J)
105 J=J+1
      K=IST(1)
      DO 110 M=1,NMR
      SUM1=SUM1+F(IST(10),K)
      SUM2=SUM2+F(IST(8),K)

110 K=K+1
      F(IST(10),IST(19))=1.0-SUM1-F(IST(10),IST(12))
      F(IST(8),IST(19))=1.0-SUM2
C
C PL SHELL
      F(IST(16),IST(19))=1.0
      J=IST(2)
      SUM1=0.0
      SUM2=0.0
      DO 115 L=1,NMR
      SUM1=SUM1+F(IST(12),J)
      SUM2=SUM2+F(IST(14),J)
115 J=J+1
      K=IST(4)
      DO 120 M=1,NSR
      SUM1=SUM1+F(IST(12),K)
      SUM2=SUM2+F(IST(14),K)
120 K=K+1
      F(IST(12),IST(19))=1.0-SUM1-F(IST(12),IST(10))
      F(IST(14),IST(19))=1.0-SUM2
C
C SPACE
      F(IST(19),IST(19))=1.0
C
C RETURN
      END
C
C ---*---
C
C SUBROUTINE FASSIGN(IFLAG,IST,FP)
C ASSIGN VIEW FACTORS FOR PCU AND PL TO USE IN
C SOLVING COMBINED RADIATION/CONDUCTION
C COMMON/CVIEW/F(100,100)
C DIMENSION FP(4,4),IST(20)
C
C IF(IFLAG.EQ.1)THEN
C FOR PAYLOAD
      L=11
      M=18
      ELSE
C FOR PCU
      L=5
      M=17
      ENDIF
C
      K=IST(L)
      DO 5 I=1,4
      IF(I.EQ.4)K=IST(M)
      KK=IST(L)
      DO 10 J=1,4
      IF(J.EQ.4)KK=IST(M)
      FP(I,J)=F(K,KK)
      KK=KK+2
10  CONTINUE

```

```

      K=K+2
      5 CONTINUE
      RETURN
      END
C
C
C-----
      FUNCTION DTOD(R1,R2,H)
C DETERMINE DISK OF RADIUS R1 TO DISK OF RADIUS R2 VIEW FACTOR
C WITH H SEPARATION DISTANCE (REF. P.826 #21 OF SIEGEL AND HOWELL)
      H=AMAX1(H,0.0001)
      CR1=R1/H
      CR2=R2/H
      DTOD=0.0
      IF(CR1.LT.1.0E-6)RETURN
      X=1.0+(1.0+CR2*CR2)/CR1/CR1
      Y=CR2/CR1
      DTOD=0.5*(X-(X*X-4.0*Y*Y)**0.5)
      RETURN
      END
C
C
C-----
      FUNCTION CTOD(R1,R2,Z)
C DETERMINE CYLINDER TO DISK VIEW FACTOR (USES VIEW FACTOR ALGEBRA
C ALONG WITH #28, P.828 OF SIEGEL AND HOWELL)
C R1 IS CYLINDER RADIUS, R2 IS DISK RADIUS
C CYLINDER IS ADJACENT AND PERPENDICULAR TO DISK
C Z IS LENGTH OF CYLINDER
      R=R2/R1
      IF(R.LT.1.0001)THEN
        CTOD=0.0
        RETURN
      ELSE
        ENDF
        XL=Z/R1
        A=XL*XL+R*R-1.0
        B=XL*XL-R*R+1.0
        C1=((A+2.0)**2-4.0*R*R)**0.5*ACOS(B/R/A)+B*ASIN(1.0/R)
        1-1.570796327*A
        C2=ACOS(B/A)-C1*0.5/XL
        C3=1.0/R-C2/R/3.141592654
        F12=C3*R
        CTOD=0.5*(1.0-F12)
        RETURN
        END
C
C
C-----
      SUBROUTINE FRINGS(R11,R10,R21,R20,H,F)
C DETERMINE VIEW FACTORS BETWEEN RINGS BASED ON DISK TO DISK
C VIEW FACTORS AND VIEW FACTOR ALGEBRA

      F=(R10*R10*(DTOD(R10,R20,H)-DTOD(R10,R21,H))-
      1 R11*R11*(DTOD(R11,R20,H)-DTOD(R11,R21,H)))/
      2 (R10*R10-R11*R11)
      RETURN
      END
C
C
C-----
      SUBROUTINE CTORING(R1,Z1,R21,R20,H,F)
C DETERMINE VIEW FACTORS BETWEEN CYLINDER AND RING
C R1 IS CYLINDER RADIUS, Z1 IS CYLINDER LENGTH
C R21 IS RING INNER RADIUS, R20 IS RING OUTER RADIUS
C H IS SEPARATION DISTANCE
      Z1=AMAX1(Z1,0.0001)
C EXTENDED CYLINDER TO SMALL RADIUS DISK
      FF1=CTOD(R1,R21,Z1+H)
C CYLINDER TO SMALL RADIUS DISK
      FFF1=H/Z1*(FF1-CTOD(R1,R21,Z1))+FF1
C EXTENDED CYLINDER TO LARGE RADIUS DISK
      FF2=CTOD(R1,R20,Z1+H)
C CYLINDER TO LARGE RADIUS DISK
      FFF2=H/Z1*(FF2-CTOD(R1,R20,Z1))+FF2
C CYLINDER TO RING
      F=FFF2-FFF1
      RETURN
      END
C
C
C-----
      SUBROUTINE OUT1(N)
      COMMON/EMIS/EMIS(100)
      COMMON/HT/ONETPP(100),T(100),R(100),G(100)
C
      WRITE(7,150)
      150 FORMAT('1',/,12X,'NETWORK SOLUTION USING GAUSS-SIEDEL',
      1/,/,1X,'SURFACE EMISSIVITY TEMPERATURE ONETPP',/(W/SQ.M)',
      2 6X,'RADIOSITY IRRADIATION',/22X,'(KELVIN)',4X,'(W/SQ.M)',
      3 6X,'(W/SQ.M)',4X,'(W/SQ.M)',/)
C
      WRITE(7,160)(I,EMIS(I),T(I),ONETPP(I),R(I),G(I),I=1,N)
      160 FORMAT(4X,12,2X,0PF9.5,5X,F7.2,4X,1PE11.4,2X,E11.4,2X,E11.4)
C
      RETURN
      END
C
C
C-----
      SUBROUTINE OUT2(IST)
      COMMON/X/XCPCU,XCPL
      COMMON/AREA/APCUSL,APCUSC,APCUSR,APCUL,APCUC,APCUR,
      1 APLSL,APLSC,APLSR,APLL,APLC,APLR,
      2 APL,APCU,APLS,APCUS

```

```

COMMON/OUT/PMR,PSR,PPCUS,PCPU,PPLS,PPL,PCUWH,PLWH,REFPOWE,
1 PSR1,PSR2,AREAMR,AREASR,TAVGPCUS,TAVGPLS,COP,
2 TISMRT,OSMR,TISSR,TOSSR,HAPCU,HAPL,CPCU,CPL,
3 THPOWER,THPNEW
COMMON/HT/ONETPP(100),T(100),R(100),G(100)
DIMENSION IST(20)
WRITE(6,100)T(IST(17)),T(IST(6)),T(IST(8)),T(IST(10)),TAVGPCUS
100 FORMAT('1',///,4X,'PCU TEMPERATURES (K):',/,
16X,'PCU - ',3X,F8.2,/,6X,'LEFT PCU SHELL - ',F8.2,/,
26X,'CENTER PCU SHELL - ',F8.2,/,
36X,'RIGHT PCU SHELL - ',F8.2,/,
46X,'SHELL AVERAGE - ',F8.2)
WRITE(6,105)T(IST(18)),T(IST(12)),T(IST(14)),T(IST(16)),TAVGPLS
105 FORMAT(' ',///,4X,'PAYLOAD TEMPERATURES (K):',/,
16X,'PAYLOAD - ',3X,F8.2,/,6X,'LEFT PAYLOAD SHELL - ',F8.2,/,
26X,'CENTER PAYLOAD SHELL - ',F8.2,/,
36X,'RIGHT PAYLOAD SHELL - ',F8.2,/,
46X,'SHELL AVERAGE - ',F8.2)
WRITE(6,107)HAPCU,HAPL
107 FORMAT(' ',///,4X,'TOTAL HA FOR CONVECTION (W/K):',/,
16X,'PCU ACTIVE COOLING - ',1PE12.4,/,
26X,'PAYLOAD ACTIVE COOLING - ',E12.4)
WCPCU=AMAX1(CPCU,XCPCU)
WCPL=AMAX1(CPL,XCPL)
WRITE(6,108)WCPCU,WCPL
108 FORMAT(' ',///,4X,'TOTAL KA/X FOR CONDUCTION (W/K):',/,
16X,'PCU TO SHELL - ',1PE12.4,/,
26X,'PAYLOAD TO SHELL - ',E12.4)
WRITE(6,110)AREAMR,AREASR,APCUS,APCU,APLS,APL
110 FORMAT(' ',///,4X,'STRUCTURE AREAS (SQ.M):',/,
16X,'MAIN RADIATOR - ',1PE12.4,/,
26X,'SECONDARY RADIATOR - ',E12.4,/,
36X,'PCU SHELL - ',E12.4,/,
46X,'PCU - ',E12.4,/,
56X,'PAYLOAD SHELL - ',E12.4,/,
66X,'PAYLOAD - ',E12.4)
WRITE(6,115)PCUWH,PSR1,PPCUS
115 FORMAT(' ',///,4X,'WASTE HEAT GENERATED IN PCU (W) = ',1PE12.4,
1/6X,'PCU WASTE HEAT REMOVED ACTIVELY (W) = ',E12.4,/,
26X,'PCU WASTE HEAT REMOVED BY CONDUCTION TO SHELL (W) = ',
3E12.4)
WRITE(6,120)PLWH,PSR2,PPLS
120 FORMAT(' ',///,4X,'WASTE HEAT GENERATED IN PAYLOAD (W) = ',1PE12.4,
1/6X,'PAYLOAD WASTE HEAT REMOVED ACTIVELY (W) = ',E12.4,/,
26X,'PAYLOAD WASTE HEAT REMOVED BY CONDUCTION TO SHELL (W) = ',
3E12.4)
WRITE(6,125)PMR,PSR,PPCUS,PCPU,PPLS,PPL
125 FORMAT(' ',///,4X,'WASTE HEAT REMOVED BY RADIATION (W):',/,
16X,'MAIN RADIATOR - ',1PE12.4,/,
26X,'SECONDARY RADIATOR - ',E12.4,/,
36X,'PCU SHELL - ',E12.4,/,6X,'PCU - ',E12.4,/,
46X,'PAYLOAD SHELL - ',E12.4,/,6X,'PAYLOAD - ',E12.4)

POWMAX=AMAX1(THPOWER,THPNEW)
WRITE(6,130)REFPOWE,COP,POWMAX
130 FORMAT(' ',///,4X,'REFRIGERATOR ELECTRIC POWER TO COOL PAYLOAD
1 (W) = ',1PE12.4,/,4X,'REFRIGERATOR COP = ',E12.4,/,
24X,'TOTAL THERMAL POWER (W) = ',E12.4,/,
36X,/,6X,25(' '),//)

C
RETURN
END

C
C
C
C
SUBROUTINE IDOUT(N,NMR,NSR,IDSURF,IDCON)
DIMENSION IDSURF(N),IDCON(N)
WRITE(7,100)
100 FORMAT(' ',4X,'SURFACE IDENTIFICATION',/,
16X,'IDSURF = 0 - SURFACE WITH KNOWN TEMPERATURE',/,
26X,'IDSURF = 1 - SURFACE WITH KNOWN HEAT FLUX',/,
36X,'IDSURF = 2 - TWO-SIDED SURFACE WITH T(SIDE 1) =
4 T(SIDE 2) AND',/,21X,'Q(TOTAL) = Q(SIDE 1) + Q(SIDE 2)',/,
56X,'(IDCON IDENTIFIES CONNECTED SURFACES, 0 FOR NO CONNECTION)',
6///,7X,'SURFACE',8X,'IDSURF',9X,'IDCON',/)

C
DO 10 I=1,N
IF(I.LE.2*NMR)WRITE(7,105)I,IDSURF(I),IDCON(I)
IF(I.GT.2*NMR.AND.I.LE.2*NMR+2*NSR)
1WRITE(7,110)I,IDSURF(I),IDCON(I)
IF(I.GT.2*NMR+2*NSR)WRITE(7,115)I,IDSURF(I),IDCON(I)
10 CONTINUE
105 FORMAT(' ',7X,13,12X,13,12X,13,7X,'MAIN RADIATOR NODE')
110 FORMAT(' ',7X,13,12X,13,12X,13,7X,'SECONDARY RADIATOR NODE')
115 FORMAT(' ',7X,13,12X,13,12X,13)
RETURN
END

C
C
C
C
SUBROUTINE FOUT(N)
COMMON/CV/IEW/F(100,100)
WRITE(7,100)
100 FORMAT(' ',1/6X,/,7X,'F(I,J)',6X,'F(J,I)',/)
DO 10 I=1,N
DO 20 J=1,N
IF(ABS(F(I,J)).GT.0.00005.OR.ABS(F(J,I)).GT.0.00005)
1WRITE(7,105)I,J,F(I,J),F(J,I)
20 CONTINUE
10 CONTINUE
105 FORMAT(' ',6X,13,4X,13,6X,F7.4,5X,F7.4)
RETURN
END

C

```

```

C -----
C
SUBROUTINE ROUT(NMR, NSR, TNMR, TNSR, TSMR, TSSR, POAMR, POASR,
1 RMR, RSR, AMR, ASR, RNMR, RNSR)
COMMON/OUT/PMR, PSR, PPCUS, PPCU, PPLS, PPL, PCUWH, PLWH, REFPOWE.
1 PSR1, PSR2, AREAMR, AREASR, TAVGPCUS, TAVGPLS, COP,
2 TISMUR, TOSMR, TISSR, TOSSR, HAPCU, HAPL, CPCU, CPL,
3 THPOWER, THPNEW
DIMENSION TNMR(NMR), TNSR(NSR), TSMR(NMR), TSSR(NSR)
DIMENSION POAMR(NMR), POASR(NSR), RMR(NMR+1), RSR(NSR+1)
DIMENSION AMR(NMR), ASR(NSR), RNMR(NMR), RNSR(NSR)
WRITE(6,100)RMR(1),RMR(NMR+1),TISMUR,TOSMR
100 FORMAT(' ',3X,'MAIN-RADIATOR NODE OUTPUT',/,
111X,'INSIDE/OUTSIDE RADII (M) = ',F8.3,/,F8.3,/,
211X,'INSIDE/OUTSIDE TEMPERATURES (K) = ',F8.3,/,F8.3,/,
35X,'NODE ',3X,'RADIUS (M) ',3X,'AREA (SQ.M) ',4X,'TEMP (K) ',
44X,'TEFF (K) ',6X,'POWER (W) ',/)
C
DO 10 I=1,NMR
P=POAMR(I)*AMR(I)
10 WRITE(6,115)I,RNMR(I),AMR(I),TNMR(I),TSMR(I),P
C
WRITE(6,105)RSR(1),RSR(NSR+1),TISSR,TOSSR
105 FORMAT(' ',/,/,/,3X,'SECONDARY-RADIATOR NODE OUTPUT',/,
111X,'INSIDE/OUTSIDE RADII (M) = ',F8.3,/,F8.3,/,
211X,'INSIDE/OUTSIDE TEMPERATURES (K) = ',F8.3,/,F8.3,/,
35X,'NODE ',3X,'RADIUS (M) ',3X,'AREA (SQ.M) ',4X,'TEMP (K) ',
44X,'TEFF (K) ',6X,'POWER (W) ',/)
C
DO 20 I=1,NSR
P=POASR(I)*ASR(I)
20 WRITE(6,115)I,RNSR(I),ASR(I),TNSR(I),TSSR(I),P
C
115 FORMAT(' ',4X,13,4X,2(F8.3,5X),1X,2(F8.2,4X),1PE12.4)
WRITE(6,120)
120 FORMAT(' ',/,/,10X,20('*-*'),/)
RETURN
END
C
C -----
C

```



PCU TEMPERATURES (K) :

PCU - 488.12  
LEFT PCU SHELL - 459.17  
CENTER PCU SHELL - 489.85  
RIGHT PCU SHELL - 487.53  
SHELL AVERAGE - 485.75

PAYLOAD TEMPERATURES (K) :

PAYLOAD - 474.75  
LEFT PAYLOAD SHELL - 508.12  
CENTER PAYLOAD SHELL - 468.43  
RIGHT PAYLOAD SHELL - 455.46  
SHELL AVERAGE - 471.80

TOTAL HA FOR CONVECTION (W/K) :

PCU ACTIVE COOLING - 0.0000E+00  
PAYLOAD ACTIVE COOLING - 2.0378E+05

TOTAL KA/X FOR CONDUCTION (W/K) :

PCU TO SHELL - 2.4514E+05  
PAYLOAD TO SHELL - 4.4273E+05

STRUCTURE AREAS (SQ.M) :

MAIN RADIATOR - 1.9062E+03  
SECONDARY RADIATOR - 6.0873E+03  
PCU SHELL - 4.0212E+02  
PCU - 2.4504E+02  
PAYLOAD SHELL - 6.2832E+02  
PAYLOAD - 4.0212E+02

WASTE HEAT GENERATED IN PCU (W) = 5.0000E+05

PCU WASTE HEAT REMOVED ACTIVELY (W) = 0.0000E+00  
PCU WASTE HEAT REMOVED BY CONDUCTION TO SHELL (W) = 4.9029E+05

WASTE HEAT GENERATED IN PAYLOAD (W) = 9.0000E+06

PAYLOAD WASTE HEAT REMOVED ACTIVELY (W) = 8.1000E+06  
PAYLOAD WASTE HEAT REMOVED BY CONDUCTION TO SHELL (W) = 8.8545E+05

WASTE HEAT REMOVED BY RADIATION (W) :

MAIN RADIATOR - 3.0000E+07  
SECONDARY RADIATOR - 8.1000E+06  
PCU SHELL - 4.9029E+05  
PCU - 1.4547E+04  
PAYLOAD SHELL - 8.8545E+05  
PAYLOAD - 1.4547E+04

.....

## SURFACE IDENTIFICATION

IDSURF = 0 - SURFACE WITH KNOWN TEMPERATURE  
 IDSURF = 1 - SURFACE WITH KNOWN HEAT FLUX  
 IDSURF = 2 - TWO-SIDED SURFACE WITH  $T(\text{SIDE 1}) = T(\text{SIDE 2})$  AND  
 $Q(\text{TOTAL}) = Q(\text{SIDE 1}) + Q(\text{SIDE 2})$   
 (IDCON IDENTIFIES CONNECTED SURFACES; 0 FOR NO CONNECTION,  
 NEGATIVE FOR SECOND SIDE OF TWO-SIDED SURFACE)

SURFACE	IDSURF	IDCON	
1	0	4	MAIN RADIATOR NODE
2	0	5	MAIN RADIATOR NODE
3	0	6	MAIN RADIATOR NODE
4	0	-1	MAIN RADIATOR NODE
5	0	-2	MAIN RADIATOR NODE
6	0	-3	MAIN RADIATOR NODE
7	0	11	SECONDARY RADIATOR NODE
8	0	12	SECONDARY RADIATOR NODE
9	0	13	SECONDARY RADIATOR NODE
10	0	14	SECONDARY RADIATOR NODE
11	0	-7	SECONDARY RADIATOR NODE
12	0	-8	SECONDARY RADIATOR NODE
13	0	-9	SECONDARY RADIATOR NODE
14	0	-10	SECONDARY RADIATOR NODE
15	2	16	PCU SHELL LEFT END (INSIDE)
16	2	-15	PCU SHELL LEFT END (OUTSIDE)
17	2	18	PCU SHELL CENTER (INSIDE)
18	2	-17	PCU SHELL CENTER (OUTSIDE)
19	2	20	PCU SHELL RIGHT END (INSIDE)
20	2	-19	PCU SHELL RIGHT END (OUTSIDE)
21	2	22	PL SHELL LEFT END (INSIDE)
22	2	-21	PL SHELL LEFT END (OUTSIDE)
23	2	24	PL SHELL CENTER (INSIDE)
24	2	-23	PL SHELL CENTER (OUTSIDE)
25	2	26	PL SHELL RIGHT END (INSIDE)
26	2	-25	PL SHELL RIGHT END (OUTSIDE)
27	1	0	PCU
28	1	0	PAYLOAD (PL)
29	0	0	SPACE

NON-ZERO VIEW FACTORS

I	J	F(I,J)	F(J,I)
1	18	0.0543	0.2462
1	20	0.0016	0.0438
1	29	0.9441	0.0000
2	18	0.0156	0.0197
2	20	0.0001	0.0005
2	29	0.9843	0.0000
3	18	0.0127	0.0066
3	20	0.0000	0.0001
3	29	0.9873	0.0000
4	7	0.2478	0.2408
4	8	0.1650	0.1574
4	9	0.1155	0.1033
4	10	0.0862	0.0686
4	22	0.0167	0.2899
4	29	0.3687	0.0000
5	7	0.1921	0.0521
5	8	0.1613	0.0429
5	9	0.1268	0.0317
5	10	0.0998	0.0222
5	22	0.0108	0.0525
5	29	0.4093	0.0000
6	7	0.1774	0.0199
6	8	0.1576	0.0173
6	9	0.1287	0.0133
6	10	0.1035	0.0095
6	22	0.0097	0.0194
6	29	0.4232	0.0000
7	20	0.0104	0.2906
7	29	0.6769	0.0000
8	20	0.0055	0.1575
8	29	0.7768	0.0000
9	20	0.0034	0.1023
9	29	0.8484	0.0000
10	20	0.0022	0.0747
10	29	0.8976	0.0000
11	22	0.0020	0.0364
11	24	0.0743	0.2218
11	29	0.9237	0.0000
12	22	0.0001	0.0010
12	24	0.0193	0.0587
12	29	0.9807	0.0000
13	22	0.0000	0.0004
13	24	0.0096	0.0311
13	29	0.9904	0.0000
14	22	0.0000	0.0002
14	24	0.0057	0.0208
14	29	0.9943	0.0000
15	17	0.3321	0.0553
15	19	0.0366	0.0366
15	27	0.6313	0.1295
16	29	1.0000	0.0000
17	17	0.2872	0.2872
17	19	0.0553	0.3321
17	27	0.6021	0.7410

18	29	0.7274	0.0000
19	27	0.6313	0.1295
20	22	0.0235	0.0150
20	29	0.3071	0.0000
21	23	0.3226	0.0538
21	25	0.0298	0.0298
21	28	0.6476	0.1265
22	29	0.5852	0.0000
23	23	0.2550	0.2550
23	25	0.0538	0.3226
23	28	0.6375	0.7470
24	29	0.6677	0.0000
25	28	0.6476	0.1265
26	29	1.0000	0.0000
29	29	1.0000	1.0000

NETWORK SOLUTION USING GAUSS-SIEDEL

SURFACE	EMISSIVITY	TEMPERATURE (KELVIN)	QNETPP (W/SQ.M)	RADIOSITY (W/SQ.M)	IRRADIATION (W/SQ.M)
1	0.90000	549.20	4.0939E+03	4.7027E+03	6.0883E+02
2	0.90000	723.57	1.3534E+04	1.4035E+04	5.0108E+02
3	0.90000	893.99	3.2146E+04	3.2639E+04	4.9330E+02
4	0.90000	549.20	3.2170E+03	4.8001E+03	1.5831E+03
5	0.90000	723.57	1.2662E+04	1.4132E+04	1.4695E+03
6	0.90000	893.99	3.1299E+04	3.2733E+04	1.4347E+03
7	0.90000	460.63	-2.9950E+02	2.5854E+03	2.8849E+03
8	0.90000	443.20	-1.0456E+02	2.1988E+03	2.3034E+03
9	0.90000	425.73	7.6644E+01	1.8538E+03	1.7772E+03
10	0.90000	408.24	1.8230E+02	1.5544E+03	1.3721E+03
11	0.90000	460.63	1.7373E+03	2.3591E+03	6.2184E+02
12	0.90000	443.20	1.5186E+03	2.0185E+03	4.9990E+02
13	0.90000	425.73	1.2447E+03	1.7241E+03	4.7936E+02
14	0.90000	408.24	9.9310E+02	1.4643E+03	4.7121E+02
15	0.90000	459.18	-6.3371E+02	2.5906E+03	3.2243E+03
16	0.90000	459.17	1.8547E+03	2.3139E+03	4.5919E+02
17	0.90000	489.88	6.9416E+01	3.2572E+03	3.1878E+03
18	0.90000	489.85	1.1506E+03	3.1362E+03	1.9855E+03
19	0.90000	487.53	6.6968E-01	3.2026E+03	3.2019E+03
20	0.90000	487.53	1.2187E+03	3.0673E+03	1.8486E+03
21	0.90000	508.13	8.6508E+02	3.6832E+03	2.8181E+03
22	0.90000	508.12	5.4606E+02	3.7184E+03	3.1724E+03
23	0.90000	468.47	-1.1749E+02	2.7435E+03	2.8610E+03
24	0.90000	468.43	1.5276E+03	2.5598E+03	1.0323E+03
25	0.90000	455.46	-3.7299E+02	2.4809E+03	2.8539E+03
26	0.90000	455.46	1.7822E+03	2.2414E+03	4.5919E+02
27	0.80000	488.12	3.9644E+01	3.2082E+03	3.1638E+03
28	0.80000	474.75	3.6175E+01	2.8707E+03	2.8292E+03
29	1.00000	300.00	0.0000E+00	4.5919E+02	4.5919E+02

**DISTRIBUTION**

**AFAT/SAS**

Fort Walton Beach, FL 32542  
Attn: Capt. Jerry Brown

**AFISC/SNAR**

Kirtland Air Force Base  
New Mexico 87117  
Attn: Lt. Col. J. P. Joyce

**AF Astronautics Laboratory/LKCJ**

Edwards Air Force Base  
California 93523  
Attn: G. Beale

**AF Astronautics Laboratory/LKCJ**

Edwards Air Force Base  
California 93523  
Attn: F. Meade

**AF Astronautics Laboratory/LKCJ**

Edwards Air Force Base  
California 93523  
Attn: Lt. R. Henley

**AF Astronautics Laboratory/LKCJ**

Edwards Air Force Base  
California 93523  
Attn: Major E. Houston

**AFWAL/AA**

Wright-Patterson AFB  
Ohio 45433  
Attn: Dick Renski

**AFWAL/POOS**

Wright-Patterson AFB  
Ohio 45433  
Attn: E. B. Kennel

**AFWAL/POOC-1**

Bldg. 450  
Wright-Patterson AF Base  
Ohio 45433  
Attn: R. Thibodeau

**AFWAL/POO**

Aeronautical Laboratory  
Wright-Patterson AFB  
Ohio 45433  
Attn: W. Borger

**AFWAL/POOA**

Aeronautical Laboratory  
Bldg. 18  
Wright-Patterson AFB  
Ohio 45433  
Attn: P. Colegrove

**AFWAL/POOC-1**

Aeronautical Laboratory  
Bldg. 450  
Wright-Patterson AFB  
Ohio 45433  
Attn: D. Massie

**AFWAL/POOC-1**

Aeronautical Laboratory  
Wright-Patterson AFB  
Ohio 45433  
Attn: C. Oberly

**AFWAL/POOC-1**

Aeronautical Laboratory  
Wright-Patterson AFB  
Ohio 45433  
Attn: T. Mahefky

**AFWAL/POOS**

Wright-Patterson AFB  
Ohio 45433  
Attn: J. Beam

**AFWAL/POOC-1**

Power Components Branch  
Wright Patterson AFB  
Ohio 45433-6563

**AFWAL/POOC**

Aeronautical Laboratory  
Bldg. 18  
Wright-Patterson AFB  
Ohio 45433  
Attn: Major Seward

**AFWL/AFSC**

Kirtland Air Force Base  
New Mexico 87117  
Attn: M. J. Schuller

**AFWL/AW**

Kirtland AFB  
New Mexico 87117  
Attn: D. Kelleher

AFWL/AWYS  
Kirtland Air Force Base  
New Mexico 87117  
Attn: Lt. Col. Jackson

AFWL/AWYS  
Kirtland Air Force Base  
New Mexico 87117  
Attn: Major D. R. Boyle

HQ AFSPACECOM/XPXIS  
Peterson Air Force Base  
Colorado 80914-5001  
Attn: Lt. Col. F. Lawrence

HQ USAF/RD-D  
Washington, DC 20330-5042  
Attn: Maj. P. Talty

Aerospace Corporation  
P. O. Box 9113  
Albuquerque, NM 87119  
Attn: W. Zelinsky

Aerospace Corporation  
P. O. Box 9113  
Albuquerque, NM 87119  
Attn: W. Blocker

Aerospace Corporation  
P. O. Box 9113  
Albuquerque, NM 87119  
Attn: M. Firmin

Aerospace Corporation  
P. O. Box 92957  
El Segundo, CA 90009  
Attn: P. Margolis

Air Force Center for Studies  
and Analyses/SASD  
The Pentagon, Room ID-431  
Washington, DC 20330-5420  
Attn: W. Barattino, AFCSA/SASD

Air Force Foreign Technology Div  
TQTD  
Wright-Patterson AFB  
Ohio 45433-6563  
Attn: B. L. Ballard

Air Force Foreign Technology Div.  
TQTD  
Wright-Patterson AFB  
Ohio 45433-6563  
Attn: K. W. Hoffman

Air Force Space Technology Center  
SWL  
Kirtland AFB, NM 87117-6008  
Attn: Capt. M. Brasher

Air Force Space Technology Center  
SWL  
Kirtland AFB, NM 87117-6008  
Attn: J. DiTucci

Air Force Space Technology Center  
SWL  
Kirtland AFB, NM 87117-6008  
Attn: Capt. E. Fornoles

Air Force Space Technology Center  
TP  
Kirtland AFB, NM 87117-6008  
Attn: M. Good

Air Force Space Technology Center  
XLP  
Kirtland AFB, NM 87117-6008  
Attn: A. Huber

Air Force Space Technology Center  
SWL  
Kirtland AFB, NM 87117-6008  
Attn: S. Peterson

ANSER Corp.  
Crystal Gateway 3  
1225 Jefferson Davis Highway #800  
Arlington, VA 22208  
Attn: K. C. Hartkay

Argonne National Laboratory  
9700 S. Cass Avenue  
Argonne, IL 60439  
Attn: S. Bhattacharyya

Argonne National Laboratory  
9700 S. Cass Avenue  
Argonne, IL 60439  
Attn: D. C. Fee

Argonne National Laboratory  
9700 S. Cass Avenue  
Argonne, IL 60439  
Attn: K. D. Kuczen

Argonne National Laboratory  
9700 S. Cass Avenue  
Argonne, IL 60439  
Attn: R. A. Lewis

Argonne National Laboratory  
9700 S. Cass Avenue  
Argonne, IL 60439  
Attn: D. C. Wade

Auburn University  
202 Sanform Hall  
Auburn, AL 36849-3501  
Attn: Dr. T. Hyder

Auburn University  
231 Leach Center  
Auburn, AL 36849-3501  
Attn: F. Rose

Avco Research Laboratory  
2385 Revere Beach Pkwy  
Everett, Mass. 02149  
Attn: D. W. Swallow

Babcock & Wilcox  
Nuclear Power Division  
3315 Old Forest Road  
P.O. Box 10935  
Lynchburg, VA 24506-0935  
Attn: B. J. Short

Battelle Pacific Northwest Lab.  
P. O. Box 999  
Richland, WA 99352  
Attn: J. O. Barner

Battelle Pacific Northwest Lab.  
P. O. Box 999  
Richland, WA 99352  
Attn: L. Schmid

Battelle Pacific Northwest Lab.  
P. O. Box 999  
Richland, WA 99352  
Attn: E. P. Coomes

Battelle Pacific Northwest Lab  
Battelle Boulevard  
Richland, WA 99352  
Attn: B. M. Johnson

Battelle Pacific Northwest Lab.  
P. O. Box 999  
Richland, WA 99352  
Attn: W. J. Krotiuk

Battelle Pacific Northwest Lab.  
P. O. Box 999  
Richland, WA 99352  
Attn: R. D. Widrig

Boeing Company  
P.O. Box 3999  
MS 8K-30  
Seattle, WA 98124-2499  
Attn: A. Sutey

Boeing Company  
Boeing Aerospace System  
P.O. Box 3707  
Seattle, WA 98124  
Attn: K. Kennerud

Brookhaven National Laboratory  
P.O. Box 155  
Upton, NY 11973  
Attn: T. Bowden

Brookhaven National Laboratory  
P.O. Box 155  
Upton, NY 11973  
Attn: H. Ludewig

Brookhaven National Laboratory  
P.O. Box 155  
Upton, NY 11973  
Attn: W. Y. Kato

Brookhaven National Laboratory  
P.O. Box 155  
Bldg. 701, Level 143  
Upton, NY 11973  
Attn: J. Powell

California Inst. of Technology  
Jet Propulsion Laboratory  
4800 Oak Grove Drive  
Pasadena, CA 91109  
Attn: V. C. Truscillo

California Inst. of Technology  
Jet Propulsion Laboratory  
4800 Oak Grove Drive  
Pasadena, CA 91109  
Attn: P. Bankston

California Inst. of Technology  
Jet Propulsion Laboratory  
4800 Oak Grove Drive  
Pasadena, CA 91109  
Attn: E. P. Framan

California Inst. of Technology  
Jet Propulsion Laboratory  
4800 Oak Grove Drive  
Pasadena, CA 91109  
Attn: L. Isenberg

California Inst. of Technology  
Jet Propulsion Laboratory  
4800 Oak Grove Drive  
Pasadena, CA 91109  
Attn: J. Mondt

DARPA  
1400 Wilson Blvd.  
Arlington, VA 22209  
Attn: P. Kemmey

DCSCON Consulting  
4265 Drake Court  
Livermore, CA 94550  
Attn: D. C. Sewell

Defense Nuclear Agency  
6801 Telegraph Road  
Alexandria, VA 22310-3398  
Attn: J. Farber/RAEV

DNA/RAEV  
6801 Telegraph Road  
Alexandria, VA 22310-3398  
Attn: J. Foster

EG&G Idaho, Inc./INEL  
P.O. Box 1625  
Idaho Falls, ID 83415  
Attn: R. Rice

EG&G Idaho, Inc./INEL  
P.O. Box 1625  
Idaho Falls, ID 83415  
Attn: J. Dearien

EG&G Idaho, Inc./INEL  
P.O. Box 1625  
Idaho Falls, ID 83415  
Attn: M. L. Stanley

EG&G Idaho, Inc./INEL  
P.O. Box 1625  
Idaho Falls, ID 83415  
Attn: R. D. Struthers

EG&G Idaho, Inc./INEL  
P.O. Box 1625  
Idaho Falls, ID 83415  
Attn: J. F. Whitbeck

EG&G Idaho, Inc./INEL  
P.O. Box 1625  
Idaho Falls, ID 83415  
Attn: P. W. Dickson

EG&G Idaho, Inc./INEL  
P.O. Box 1625  
Idaho Falls, ID 83415  
Attn: J. W. Henscheid

Ford Aerospace Corporation  
Aeronutronic Div.  
Ford Road, P.O. Box A  
Newport Beach, CA 92658-9983  
Attn: V. Pizzuro

GA Technologies  
P.O. Box 85608  
San Diego, CA 92138  
Attn: H. J. Snyder

GA Technologies  
P.O. Box 85608  
San Diego, CA 92138  
Attn: C. Fisher

GA Technologies  
P.O. Box 85608  
San Diego, CA 92138  
Attn: R. Dahlberg

Garrett Fluid Systems Co.  
P.O. Box 5217  
Phoenix, AZ  
Attn: Robert Boyle

General Electric Company  
P. O. Box 8555  
Astro Systems  
Philadelphia, PA 19101  
Attn: R. J. Katucki

General Electric Corp/NSTO  
310 DeGuigne Drive  
Sunnyvale, CA 9048  
Attn: C. Cowan

General Electric NSTO  
310 DeGuigne Drive  
Sunnyvale, CA 90486  
Attn: E. E. Gerrels

General Electric NSTO  
310 DeGuigne Drive  
Sunnyvale, CA 90486  
Attn: H. S. Bailey

General Electric-SCO  
P. O. Box 8555  
Astro Systems  
Philadelphia, PA 19101  
Attn: J. Chan

General Electric  
P. O. Box 8555  
Bldg. 100, Rm M2412  
Astro Systems  
Philadelphia, PA 19101  
Attn: J. Hnat

General Electric  
P. O. Box 8555  
Astro Systems  
Philadelphia, PA 19101  
Attn: R. D. Casagrande

General Electric  
P. O. Box 8555  
Astro Systems  
Philadelphia, PA 19101  
Attn: W. Chiu

Grumman Aerospace Corporation  
M/S B20-05  
Bethpage, NY 11714  
Attn: J. Belisle

Hanford Engineering Dev. Lab  
Post Office Box 1970  
Richland, WA 99352  
Attn: D. S. Dutt

House of Representatives Staff  
Space and Technology Committee  
2320 Rayburn Building  
Washington, DC 20515  
Attn: Tom Weimer

Idaho National Engineering  
Laboratory  
P. O. Box 1625  
Idaho Fall, ID 83414  
Attn: W. H. Roack

Innovative Nuclear Space Pwr.Inst.  
202 NSC  
University of Florida  
Gainesville, FL 32611  
Attn: N. J. Diaz

International Energy Assoc. Ltd.  
1717 Louisiana NE  
Suite 202  
Albuquerque, NM 87110  
Attn: G. B. Varnado

Lawrence Livermore National Lab.  
P. O. Box 808  
Livermore, CA 94550  
Attn: Lynn Cleland, MS L-144

Lawrence Livermore National Lab.  
P. O. Box 808  
Livermore, CA 94550  
Attn: C. E. Walter, MS L-144

Los Alamos National Laboratory  
P. O. Box 1663  
Los Alamos, NM 87545  
Attn: T. Trapp, MS-E561

Los Alamos National Laboratory  
P. O. Box 1663  
Los Alamos, NM 87545  
Attn: R. Hardie, MS-F611

Los Alamos National Laboratory  
P. O. Box 1663  
Los Alamos, NM 87545  
Attn: C. Bell, MS A145

Los Alamos National Laboratory  
P. O. Box 1663  
Los Alamos, NM 87545  
Attn: R. J. LeClaire

Los Alamos National Laboratory  
P. O. Box 1663  
Los Alamos, NM 87545  
Attn: S. Jackson, MS-F611

Los Alamos National Laboratory  
P. O. Box 1663  
Los Alamos, NM 87545  
Attn: J. Metzger

Los Alamos National Laboratory  
P. O. Box 1663  
Los Alamos, NM 87545  
Attn: C. W. Watson, MS-F607

Los Alamos National Laboratory  
P. O. Box 1663  
Los Alamos, NM 87545  
Attn: Don Reid, MS-H811

Los Alamos National Laboratory  
P. O. Box 1663  
Los Alamos, NM 87545  
Attn: R. Bohl, MS-K551

Los Alamos National Laboratory  
P. O. Box 1663  
Los Alamos, NM 87545  
Attn: D. R. Bennett

Los Alamos National Laboratory  
P. O. Box 1663  
Los Alamos, NM 87545  
Attn: W. L. Kirk

Los Alamos National Laboratory  
P. O. Box 1663  
Los Alamos, NM 87545  
Attn: M. Merrigan

Los Alamos National Laboratory  
P. O. Box 1663  
Los Alamos, NM 87545  
Attn: T. P. Suchocki

Los Alamos National Laboratory  
P. O. Box 1663  
Los Alamos, NM 87545  
Attn: L. H. Sullivan

Martin Marietta Corp.  
P. O. Box 179  
Denver, CO 80201  
Attn: R. Giellis

Martin Marietta Corp.  
P. O. Box 179  
Denver, CO 80201  
Attn: R. Zercher  
MSL8060

Massachusetts Institute of  
Technology  
1328 Albany Street  
Cabridge, MA 02139  
Attn: J. A. Bernard

NASA Lewis Research Center  
21000 Brookpark Road  
Cleveland, OH 44135  
Attn: Barbara McKissock, MS 301-5

NASA Lewis Research Center  
21000 Brookpark Road  
Cleveland, OH 44135  
Attn: A. Juhasz, MS 301-5

NASA Lewis Research Center  
21000 Brookpark Road  
Cleveland, OH 44135  
Attn: J. Smith, MS 301-5

NASA Lewis Research Center  
21000 Brookpark Road  
Cleveland, OH 44135  
Attn: H. Bloomfield, MS 301-5

NASA Lewis Research Center  
21000 Brookpark Road  
Cleveland, OH 44135  
Attn: C. Purvis, MS 203-1

NASA Lewis Research Center  
21000 Brookpark Road  
Cleveland, OH 44135  
Attn: D. Bents, MS 301-5

NASA Lewis Research Center  
21000 Brookpark Road  
Cleveland, OH 44135  
Attn: I. Myers, MS 301-2

NASA Lewis Research Center  
21000 Brookpark Road  
Cleveland, OH 44135  
Attn: G. Schwarze, MS 301-2

NASA Lewis Research Center  
21000 Brookpark Road  
Cleveland, OH 44135  
Attn: J. Sovie, MS 301-5

NASA Lewis Research Center  
21000 Brookpark Road  
Cleveland, OH 44135  
Attn: Barbara Jones, MS 301-5

National Research Council  
Energy Engineering Board  
Commission on Engineering  
and Technical Systems  
2101 Constitution Avenue  
Washington, DC 20418  
Attn: R. Cohen

Naval Research Laboratory  
Washington, DC 20375-5000  
Attn: R. L. Eilbert

Naval Research Laboratory  
Washington, DC 20375-5000  
Attn: I. M. Vitkovitsky

Naval Space Command  
Dahlgren, VA 22448  
Attn: Commander R. Nosco

Naval Space Command  
N5  
Dahlgren, VA 22448  
Attn: Maj. J. Wiley

Naval Space Command  
Dahlgren, VA 22448  
Attn: Mr. B. Meyers

Naval Surface Weapons Center  
Dahlgren, VA 22448-5000  
Attn: R. Gripshoven-F12

Naval Surface Weapons Center  
Dahlgren, VA 22448-5000  
Attn: R. Dewitt-F12

Naval Surface Weapons Center  
White Oak Laboratory  
Silver Springs, MD 20903-500  
MC R-42  
Attn: B. Maccabee

Nichols Research Corp.  
2340 Alamo Street, SE  
Suite 105  
Albuquerque, NM 87106  
Attn: R. Weed

Oak Ridge National Laboratory  
P. O. Box Y  
Bldg. 9201-3, MS-7  
Oak Ridge, TN 37831  
Attn: J. P. Nichols

Oak Ridge National Laboratory  
P. O. Box Y  
Bldg. 9201-3, MS-7  
Oak Ridge, TN 37831  
Attn: D. Bartine

Oak Ridge National Laboratory  
P. O. Box X  
Oak Ridge, TN 37831  
Attn: H. W. Hoffman

Oak Ridge National Laboratory  
P. O. Box Y  
Bldg. 9201-3, MS-7  
Oak Ridge, TN 37831  
Attn: R. H. Cooper, Jr.

Oak Ridge National Laboratory  
P. O. Box Y  
Bldg. 9201-3, MS-7  
Oak Ridge, TN 37831  
Attn: J. C. Moyers

Oak Ridge National Laboratory  
P. O. Box Y  
Oak Ridge, TN 37831  
Attn: M. Olszewski

Oak Ridge National Laboratory  
P. O. Box Y  
Bldg. 9201-3, MS-7  
Oak Ridge, TN 37831  
Attn: M. Siman-Tov

Oak Ridge National Laboratory  
P. O. Box Y  
Bldg. 9201-3, MS-7  
Oak Ridge, TN 37831  
Attn: F. W. Wiffen

RADC/OCTP  
Griffiss AFB  
New York 13441  
Attn: R. Gray

Riverside Research Institute  
1701 No. Ft. Meyers Drive  
Suite 700  
Arlington, VA 22209  
Attn: J. Feig

Science Applications, Inc.  
505 Marquette Avenue NW  
Albuquerque, NM 87102  
Attn: D. Buden

Science & Engineering Associates  
6301 Indian School Road, NE  
Albuquerque, NM 87110  
Attn: G. L. Zigler

SDI Organization  
The Pentagon  
Washington, DC 20301-7100  
Attn: R. Verga

SDI Organization  
The Pentagon  
Washington, DC 20301-7100  
Attn: R. Wiley

SDI/SLKT  
The Pentagon  
1717 H. St. NW  
Washington, D. C. 20301  
Attn: C. Northrup

SDIO/DE  
Washington, DC 20301-7100  
Attn: Dr. J. Hammond

SDIO/IST  
Washington, DC 20301-7100  
Attn: Dr. L. Cavery

SDIO/KE  
The Pentagon  
Washington, DC 20301-7100  
Attn: Col. R. Ross

SDIO/KE  
The Pentagon  
Washington, DC 20301-7100  
Attn: Maj. R. X. Lenard

SDIO/SATKA  
Washington, DC 20301-7100  
Attn: Col. Garry Schnelzer

SDIO/SY  
Washington, DC 20301-7100  
Attn: Dr. C. Sharn

SDIO/SY  
Washington, DC 20301-7100  
Attn: Col. J. Schofield

SDIO/SY  
Washington, DC 20301-7100  
Attn: Col. J. Graham

SDIO/SY  
Washington, DC 20301-7100  
Attn: Capt. J. Doegan

Space Power, Inc.  
253 Humbolt Court  
Sunnyvale, CA 94089  
Attn: J. R. Wetch

State University of New York  
at Buffalo  
Dept. of Elec. Engineering  
312 Bonner Avenue  
Buffalo, NY 14260  
Attn: Jim Sargeant

TRW  
One Space Park  
Redondo Beach, CA 90278  
Attn: R. Hammel

TRW  
One Space Park  
Redondo Beach, CA 90278  
Attn: T. Fitzgerald

TRW  
One Space Park  
Redondo Beach, CA 90278  
Attn: C. Garner

TRW-ATD  
One Space Park  
Redondo Beach, CA 90278  
Attn: B. Glasgow

TRW  
One Space Park  
Redondo Beach, CA 90278  
Attn: A. D. Schoenfeld

Teledyne Brown Engineering  
Cummings Research Park  
Huntsville, AL 35807  
Attn: Dan DeLong

Texas A&M University  
Nuclear Engineering Dept.  
College Station, TX 77843-3133  
Attn: F. Best

Texas Tech. University  
Dept. of Electrical Engr.  
Lubbock, TX 79409  
Attn: Dr. W. Portnoy

U. S. Army ARDC  
Building 329  
Picatinny Arsenal  
New Jersey 87806-5000  
Attn: SMCAR-SSA-E

U. S. Army Belvoir RDE Center  
Fort Belvoir, VA 22060-5606  
Attn: Dr. L. Amstutz-STRABE-FGE

U. S. Army Lab. Com.  
SLKET/ML  
Pulse Power Technology Branch  
Fort Monmouth, NJ 07703-5000  
Attn: S. Levy

U. S. Army Lab. Com.  
SLKET/ML  
Pulse Power Technology Branch  
Fort Monmouth, NJ 07703-5000  
Attn: N. Wilson

U. S. Army Strategic Defense Com.  
106 Wynn Drive  
Huntsville, AL 35807  
Attn: C. Cooper

U. S. Army Strategic Defense Com.  
106 Wynn Drive  
Huntsville, AL 35807  
Attn: G. Edlin

U. S. Army Strategic Defense Com.  
106 Wynn Drive  
Huntsville, AL 35807  
Attn: R. Hall

U. S. Army Strategic Defense Com.  
106 Wynn Drive  
Huntsville, AL 35807  
Attn: E. L. Wilkinson

U. S. Army Strategic Defense Com.  
106 Wynn Drive  
Huntsville, AL 35807  
Attn: D. Bouska

U. S. Army Strategic Defense Com.  
106 Wynn Drive  
Huntsville, AL 35807  
Attn: W. Sullivan

U. S. Army Strategic Defense Com.  
106 Wynn Drive  
Huntsville, AL 35807  
Attn: F. King

U. S. Department of Energy  
Chicago Operations Office  
9800 S. Cass Avenue  
Argonne, IL 60439  
Attn: J. L. Hooper

U. S. Department of Energy  
NE-52  
GTN  
Germantown, MD 20545  
Attn: J. Warren

U. S. Department of Energy  
NE-54  
F415/GTN  
Germantown, MD 20545  
Attn: E. Wahlquist

U. S. Department of Energy  
NE-521  
Germantown, MD 20874  
Attn: D. Bennett

U. S. Department of Energy  
San Francisco Operations Office  
1333 Broadway Ave,  
Oakland, CA 94612  
Attn: J. K. Hartman

U. S. Department of Energy  
SAN - ACR Division  
1333 Broadway  
Oakland, CA 94612  
Attn: J. Krupa

U. S. Department of Energy  
SAN - ACR Division  
1333 Broadway  
Oakland, CA 94612  
Attn: W. Lambert

U. S. Department of Energy  
SAN - ACR Division  
1333 Broadway  
Oakland, CA 94612  
Attn: J. Zielinski

U. S. Department of Energy  
Pittsburgh Energy Tech. Center  
P.O. Box 18288  
Pittsburgh, PA 15236  
Attn: G. Staats (PM-20)

U. S. Department of Energy  
NE-54  
Washington, DC 20545  
Attn: I. Helms

U. S. Department of Energy  
Oak Ridge Operations Office  
P.O. Box E  
Oak Ridge, TN 37830  
Attn: E. E. Hoffman

U. S. Department of Energy  
Washington, DC 20545  
Attn: S. J. Lanes

U. S. Department of Energy  
MA 206  
Washington, DC 20545  
Attn: J. P. Lee

U. S. Department of Energy  
San Francisco Operations Office  
1333 Broadway Avenue  
Oakland, CA 94612  
Attn: S. L. Samuelson

U. S. Department of Energy  
ALO/ETD  
P.O. Box 5400  
Albuquerque, New Mexico 87115  
Attn: R. Holton

U. S. Department of Energy  
ALO/ETD  
P.O. Box 5400  
Albuquerque, New Mexico 87115  
Attn: C. Quinn

U. S. Department of Energy/Idaho  
785 DOE Place  
Idaho Falls, ID 83402  
Attn: P. J. Dirkmaat

United Technologies  
International Fuel Cells  
195 Governor's Highway  
South Windsor, CT 06074  
Attn: D. McVay

United Technologies  
International Fuel Cells  
195 Governor's Highway  
South Windsor, CT 06074  
Attn: J. L. Preston, Jr.

United Technologies  
International Fuel Cells  
195 Governor's Highway  
South Windsor, CT 06074  
Attn: J. C. Trocciola

University of Missouri - Rolla  
220 Engineering Research Lab  
Rolla, MO 65401-0249  
Attn: A. S. Kumar

University of New Mexico  
Chemical and Nuclear Eng.  
Department  
Albuquerque, NM 87131  
Attn: M. El-Genk

University of Wisconsin  
Fussion Technology Institute  
1500 Johnson Drive  
Madison, WI 53706-1687  
Attn: Gerald Kukinski

W. J. Schafer Associates  
1901 No. Ft. Myers Drive  
Suite 800  
Arlington, VA 22209  
Attn: P. Mace

W. J. Schafer Associates  
1901 No. Ft. Myers Drive  
Suite 800  
Arlington, VA 22209  
Attn: S. Bassett

W. J. Schafer Associates  
1901 No. Ft. Myers Drive  
Suite 800  
Arlington, VA 22209  
Attn: M. Nikolich

W. J. Schafer Associates  
1901 No. Ft. Myers Drive  
Suite 800  
Arlington, VA 22209  
Attn: J. Crissey

W. J. Schafer Associates  
2000 Randolph Road, SE  
#205  
Albuquerque, NM 87106  
Attn: D. C. Straw

W. J. Schafer Associates  
1901 No. Ft. Myers Drive  
Suite 800  
Arlington, VA 22209  
Attn: A. K. Hyder

Westinghouse Electric  
P. O. Box 158  
Madison, PA 15663-0158  
Attn: J. Chi

Westinghouse  
Advanced Energy Systems Division  
Manager, Space & Defense Program  
Route 70, Madison Exit  
Madison, PA 15663  
Attn: J. F. Wett

Westinghouse  
Advanced Energy Systems Division  
P.O. Box 158  
Madison, PA 15663  
Attn: Dr. J. W. H. Chi

Westinghouse R&D  
1310 Beulah Road  
Bldg. 501-3Y56  
Pittsburgh, PA 15235  
Attn: J. R. Repp

Westinghouse R&D  
1310 Beulah Road  
Bldg. 501-3Y56  
Pittsburgh, PA 15235  
Attn: L. Long

Westinghouse R&D  
1210 Beulah Road  
Bldg. 501-3Y56  
Pittsburgh, PA 15235  
Attn: Owen Taylor

Westinghouse Advanced Energy  
Systems Division  
P. O. Box 158  
Madison, PA 15663  
Attn: G. Farbman

Westinghouse Hanford Co.  
P. O. Box 1970  
Richland, WA 99352  
Attn: D. S. Dutt

Westinghouse Hanford Co.  
P. O. Box 1970  
Richland, WA 99352  
Attn: B. J. Makenas

1140 P. Peercy  
1200 J. P. Van Devender  
1240 K. Prestwich  
1248 M. Buttram  
1270 R. Miller  
1271 M. Clauser  
1512 D. Rader  
1800 R. Schwoebel  
1810 G. Kepler  
1830 M. Davis  
1832 W. Jones  
1832 R. Salzbrenner  
1840 R. Eagan  
2110 R. Bair  
2120 W. Dawes, Jr.  
2140 C. Gibbon  
2150 E. Graham, Jr.  
2560 J. Cutchen  
3141 S. A. Landenberger (5)  
3151 W. L. Garner (3)  
3154-1 C.H. Dalin, for DOE/OSTI (28)

6400 D. McCloskey  
6410 N. Ortiz  
6420 J. Walker  
6421 P. Pickard  
6422 J. Brockman  
6425 W. Camp  
6431 J. Philbin  
6440 D. Dahlgren  
6450 T. Schmidt  
6500 A. W. Snyder  
6510 W. Gauster  
6511 L. Cropp  
6511 M. Edenburn  
6511 D. Gallup  
6511 S. Hudson  
6511 A. Marshall  
6511 W. McCulloch  
6511 R. Pepping  
6511 F. Thome  
6512 D. Ericson (5)  
6512 M. Chu  
6512 V. Dandini  
6512 D. Dobranich (10)  
6512 P. McDaniel  
6512 F. Wyant  
8024 P. W. Dean  
8400 R. Wayne  
9000 R. Hagenruber  
9010 W. C. Hines  
9012 J. Keizur  
9012 L. Connell  
9012 R. Zazworski  
9100 R. Clem  
9110 P. Stokes  
9140 D. Rigali